UNIVERSIDADE DA CORUÑA

FACULTADE DE CIENCIAS

Bachelor of Science in Chemistry

Final Degree Project Report

Application of coordination compounds as optic sensors.

Aplicación de compostos de coordinación como sensores ópticos.

Aplicación de compuestos de coordinación como sensores ópticos.

Advisors: Elena Pazos Chantrero

Carlos Platas Iglesias

FRANCISCO JAVIER FERREIRO REY

Academic year: 2017/2018 – Call: July

Final Degree Project Report in Chemistry presented by Mr. **Francisco Javier Ferreiro Rey** at the Faculty of Science of the Universidade da Coruña.

July 2018

Acknowledgements

- To my advisors, Dr. Elena Pazos Chantrero and Dr. Carlos Platas Iglesias, for their patience and dedication during the whole project, and for sharing their gigantic wisdom. Definitely it has been an honor to have worked with you.

- To Rosa Todopoderosa and Rochi, since I entered in the lab with terrible laboratory skills, and now I can perform chromatography columns, filtrations and synthesis like a boss (more or less), all thanks to their tricks and help.

- To Dr. David Esteban Gómez, for his kindness and for acting as a co-advisor and helping me whenever I need it.

- To my peers, Angy, for making laboratory time the funniest and for not refusing to have romantic lunches with me during this whole term, and to Pablo, since we both become masters in HPLC and SPPS; and he is nice also.

THANK YOU ALL

Index

Abbreviations

Å	Angstrom
Ac	Acetyl
Ac_2O	Acetic anhydride
ACN	Acetonitrile
Allyl	Allyl ether
Boc	*Tert*-butoxycarbonyl
CH_2Cl_2	Dichloromethane
CN	Coordination number
Cyclen	1,4,7,10-tetraazacyclododecane
DCC	*N,N'*-dicyclohexylcarbodiimide
DEDTC	Diethyldithiocarbamate
DIEA	*N,N'*-diisopropylethylamine
DMF	Dimethylformamide
DOTA	1,4,7,10-tetraazacyclododecane-1,4,7,10-tetraacetate
DOTAM	1,4,7,10-tetrakis(carbamoilmethyl)-1,4,7,10-tetraazacyclododecane
ESI	Electrospray ionization
Fmoc	9-fluorenylmethoxycarbonyl
HATU	1-[Bis(dimethylamino)methylene]-1H-1,2,3-triazolo[4,5-b]pyridinium 3-oxid hexafluorophosphate
HF	Fluorhydric acid
HOBt	1-hydroxybenzotriazole
HPLC	High Performance Liquid Chromatography
MeOH	Methanol
MPLC	Medium Pressure Liquid Chromatography
MS	Mass Spectrometry
NMM	*N*-methylmorpholine
NMR	Nuclear Magnetic Resonance
$Pd(OAc)_2$	Palladium acetate
$PhSiH_3$	Phenylsilane
PPh_3	Triphenylphosphine
rt	Room temperature
SPPS	Solid Phase Peptide Synthesis
*t*Bu	*Tert*-butyl
TFA	Trifluoroacetic acid
TIS	Triisopropylsilane
TNBS	2,4,6-trinitrobenzenesulfonic acid
t_R	Retention time
δ	Chemical shift

Abstract

Nitration of tyrosine residues of proteins has been found to be related to the onset and the progression of neurodegenerative diseases such as Parkinson's. In cells, this protein modification is mediated by peroxynitrite, which is produced under oxidative stress conditions. The aim of this work is the design and synthesis of a luminescent sensor for oxidative stress. The basis is to use a lanthanide-peptide complex whose luminescence signal will increase under oxidative stress conditions, by using the generated 3-nitrotyrosine chromophore as lanthanide sensitizer.

Thus, two peptides, having the same sequence but one of them containing a nitrated tyrosine residue, were synthesized following standard Fmoc solid phase peptide synthesis protocols. In addition, two different DOTA derivative ligands were synthesized following stablished synthetic methodologies, and those were coupled to the peptides at an orthogonally deprotected Glu residue side chain, while the peptides are still attached to the solid support. The expected products were obtained, although without full completion of the reaction.

HPLC-MS and NMR were the techniques used in order to characterize the products and to follow the reactions.

Keywords: lanthanides, solid phase peptide synthesis, coordination chemistry, luminescence.

Resumen

La nitración de residuos de tirosina en proteínas está relacionada con el inicio y la progresión de enfermedades neurodegenerativas como el Parkinson. En las células, esta modificación de las proteínas es producida por moléculas de peroxinitrito, que se generan en condiciones de estrés oxidativo. El objetivo de este trabajo es el diseño y síntesis de un sensor luminiscente de estrés oxidativo. La base es usar un complejo péptido-lantánido cuya señal de luminiscencia aumentará en condiciones de estrés oxidativo, al utilizar el cromóforo 3-nitrotirosina generado como sensibilizador del lantánido.

Por lo tanto, se sintetizaron dos péptidos, que tienen la misma secuencia pero uno de ellos contiene un residuo de tirosina nitrado, siguiendo protocolos habituales de síntesis de péptidos en fase sólida utilizando la estrategia Fmoc. Además, se sintetizaron dos ligandos derivados del DOTA, siguiendo metodologías sintéticas establecidas, y estos se acoplaron a los péptidos en la cadena lateral de un residuo de Glu ortogonalmente desprotegida, mientras los péptidos todavía están unidos al soporte sólido. Se obtuvieron los productos esperados, pero sin producirse la conversión total de los productos de partida.

HPLC-MS y RMN fueron las técnicas utilizadas para caracterizar los productos y seguir las reacciones.

Palabras clave: lantánidos, síntesis de péptidos en fase sólida, química de coordinación, luminiscencia.

Resumo

A nitración de residuos de tirosina en proteínas está relacionada co inicio e a progresión de enfermidades neurodexenerativas como o Parkinson. Nas células, esta modificación das proteínas é producida por moléculas de peroxinitrito, que se xeran en condicións de estrés oxidativo. O obxectivo deste traballo é o deseño e síntese dun sensor luminescente de estrés oxidativo. A base é usar un complexo péptido-lantánido cuxa sinal de luminescencia aumentará en condicións de estrés oxidativo, ao utilizar o cromóforo 3-nitrotirosina xerado como sensibilizador do lantánido.

Polo tanto, sintetizáronse dous péptidos, que teñen a mesma secuencia pero un deles contén un residuo de tirosina nitrado, seguindo protocolos habituais de síntese de péptidos en fase sólida utilizando a estratexia Fmoc. Ademais, sintetizáronse dous ligandos derivados do DOTA, seguindo metodoloxías sintéticas establecidas, e estes acopláronse aos péptidos na cadea lateral dun residuo de Glu ortogonalmente desprotexida, mentres os péptidos aínda están unidos ao soporte sólido. Obtivéronse os produtos esperados pero sen producirse a total conversión dos produtos de partida.

HPLC-MS e RMN foron as técnicas utilizadas para caracterizar os produtos e seguir as reaccións.

Palabras chave: lantánidos, síntese de péptidos en fase sólida, química de coordinación, luminiscencia.

Introduction

Neurodegenerative Diseases and Oxidative Stress

Neurodegenerative diseases are characterized by a progressive dysfunction of the nervous system. These disorders are usually associated with the atrophy of the affected central or peripheral structures, including diseases such as Parkinson's, Alzheimer's and other dementias, as well as diseases caused by prions, among many others. In 2009, the European Union estimated that 7 million European citizens had developed this type of diseases, and that the treatment and care of these patients cost the European health services approximately 130.000 million euros only in 2005. As a consequence of the aging of European population, these data are expected to increase considerably in the coming decades. The existing treatments for neurodegenerative diseases are limited, and mainly treat the symptoms instead of treating their causes.

Parkinson's disease is the second most common neurodegenerative disorder and affects 2-3% of the population over 65 years of age. Its neuropathological characteristics include neuronal loss in specific areas of the brain, accompanied by insoluble aggregates of the α-synuclein protein.[1–3] The underlying molecular pathogenesis involves multiple pathways and mechanisms such as α-synuclein proteostasis, mitochondrial function or oxidative stress among others.

Oxidative stress is produced due to a disturbance in the balance between the concentration of reactive oxygen species (free radicals) and antioxidant defenses, which may cause protein damage and tissue injury. The most common free radicals present in biological environments include the hydroxyl radical ($^{\bullet}OH$), superoxide anion ($O_2^{\bullet-}$), transition metals such as iron and copper, nitric oxide ($NO^{\bullet}$), and peroxynitrite ($ONOO^-$)[4]; the latest of these playing a crucial role in biomolecule nitration.[4]

Peroxynitrite is a strong nitrating agent formed primarily by the reaction between the two radicals nitric oxide ($NO^{\bullet}$) and superoxide ($O_2^{\bullet-}$) in biological environments. The most representative process mediated by peroxynitrite is the nitration of tyrosine (3-nitrotyrosine), which is defined as the substitution of a hydrogen in the ortho-position of the phenolic ring by a nitro group, either in free or coupled tyrosine.[5]

Several studies have identified accumulations of α-synuclein protein with nitrated tyrosine residues in the characteristic inclusions of Parkinson's disease (Lewy bodies), evidencing a clear connection between oxidative and nitrative damage with the onset and the progression of neurodegenerative synucleinopathies.[6]

PROTEINS AND PEPTIDES

PEPTIDE BOND AND PROTEIN STRUCTURE

Peptides and proteins are biopolymers whose monomer units are α-amino acids bound each other by an amide bond (also known as peptide bond). α-amino acids are characterized for having an amine group in the α position of a carboxylic acid group, and follow the general formula of $H_2NCH(R)COOH$. In order to form peptides, repeated reactions of one carboxylic acid group of one amino acid with the amine group of another occur to give a chain of amides formed by condensation.[7]

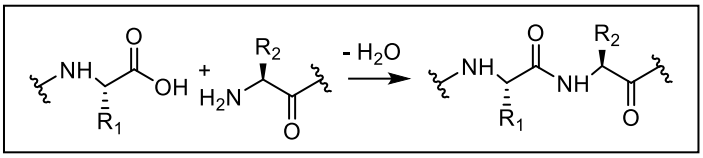

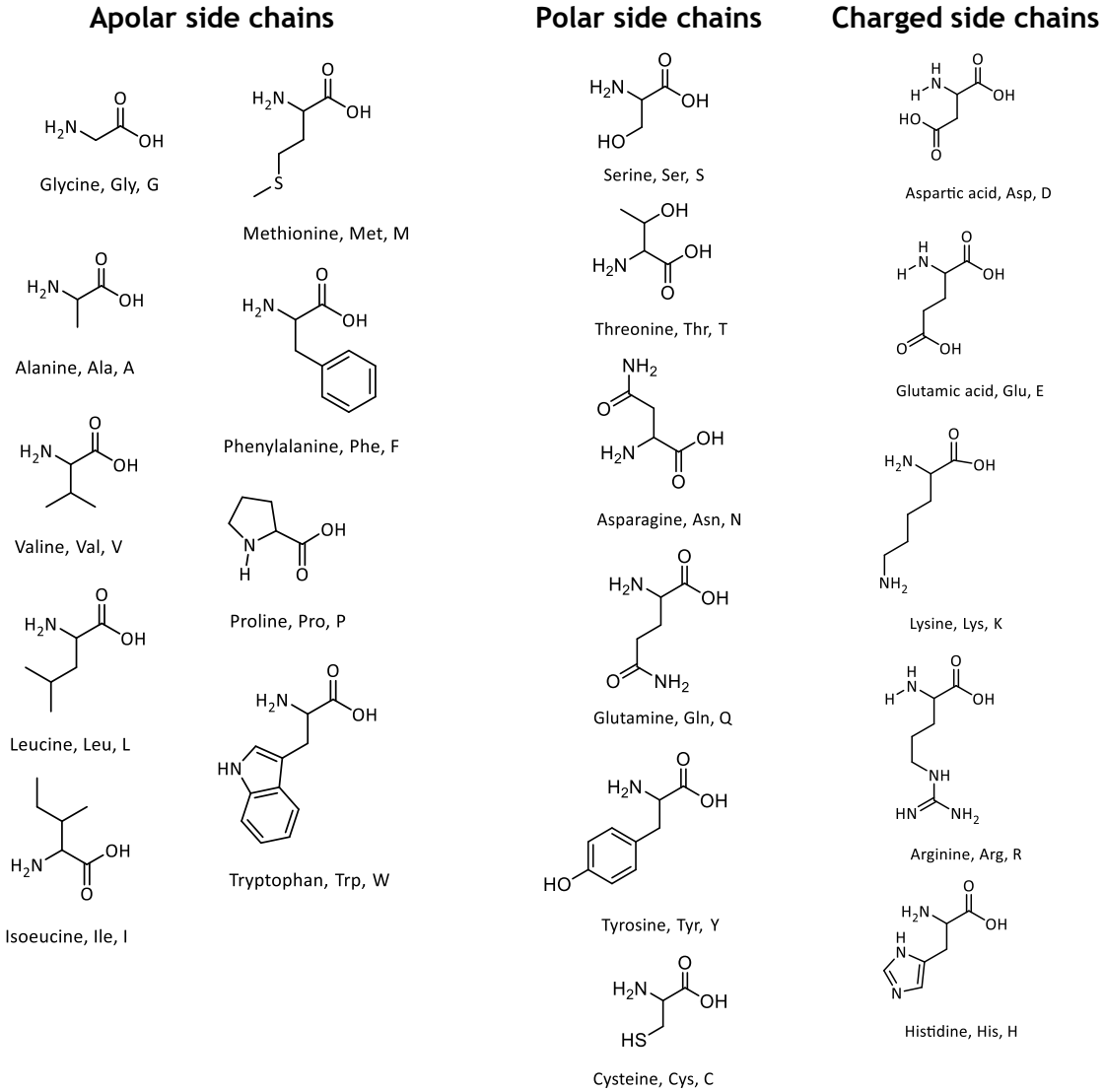

***Figure 1**. Peptide bond formation by condensation of a carboxylic acid and an amine. Structure and codes of one and three letters for the most common amino acids.*

All of these amino acids belong to the L series; therefore, they have the same stereochemistry. Depending on the side chain (R group), amino acids can be classified into three main groups: apolar (G, A, V, L, I, M, F, P, W), polar (S, T, N, Q, Y, C) and charged ones, which can be acidic (D, E) or basic (K, R, H).

It should be mentioned that a peptide bond can be represented as two resonance isomers (Figure 2). This means that the actual peptide bond is a resonance hybrid of these two isomer structures, which makes the C-N bond having a 50% of double bond character. The consequence of this is that rotation mainly occurs between Cα–C and N–Cα bonds meaning that the adjacent peptide planes (see Figure 3)[8] can rotate with respect to each other.[9]

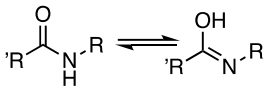

Figure 2. *Electronic isomer structure of a peptide bond.*

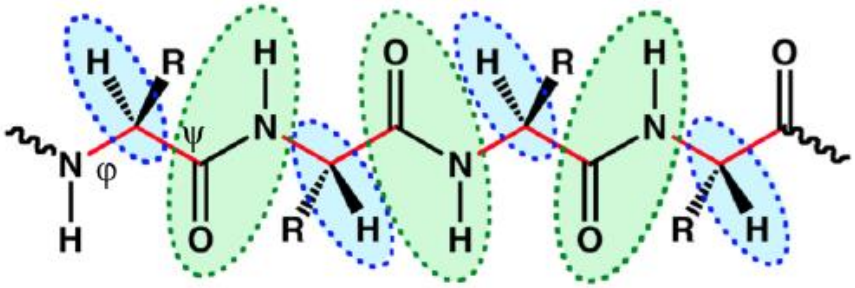

Figure 3. *Representation of the repeating amino acid units of a polypeptide chain with alternating rigid amide (green) and α-carbon planes linked by rotating ψ and ϕ bonds.*[8]

However, the idea of amino acids bonded together in a flat two-dimensional model for a polypeptide chain does not describe adequately the reality of a three-dimensional arrangement, which bears the structure of a protein. In fact, it is this complicated folding structure, which gives proteins their characteristic functional properties.

When describing the three-dimensional structure of proteins, all levels of organization should be considered. Primary structure refers to the linear sequence of amino acid residues along the polypeptide chain. Every protein is defined by a unique linear order of residues and all subsequent levels of arrangement rely on this primary level of structure.[10]

Rather than an extended configuration of a polypeptide chain, most proteins are present in a compact globular form, whose interior is a strongly hydrophobic environment. This may be a problem since polypeptides have polar groups capable of forming hydrogen bonds by the C=O and N-H groups and they cannot bond with the side chain hydrophobic groups of the molecule. Therefore, in order to bear a stable conformation, the backbone groups will bond with the same or an adjacent polypeptide backbone, arising the secondary structure.

There are two main types of secondary structures, the α-helix and the β-pleated sheet (Figure 4)[11]. In the first one, the polypeptide backbone twists into a right-handed helix in which 3.6 amino acids units are needed to perform a turn (this was deduced by Linus Pauling in 1951). This results in the C=O of each peptide bond to form a hydrogen bond with the N-H group of the fourth consecutive amino acid, forming a cylindrical structure. Meanwhile, in the β-pleated sheet, the backbone groups form a hydrogen bond to groups of an adjacent one; thus, giving the possibility to several polypeptide chains to form a single sheet. The adjacent polypeptide chain can be bonded in a parallel or in a antiparallel manner depending on the alignment of the hydrogen bonds.[12]

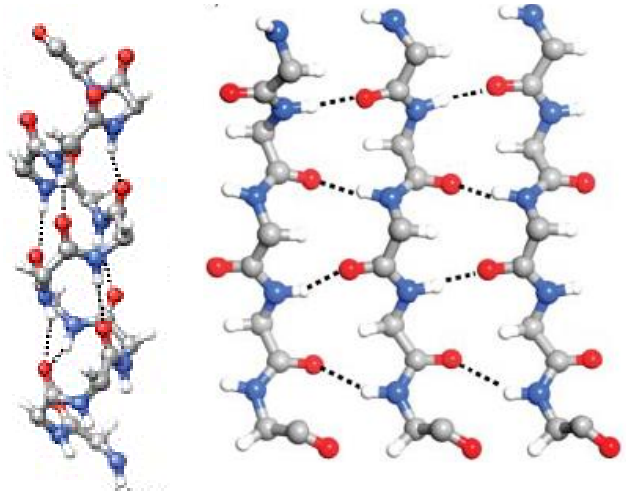

Figure 4. Left: *Representation of an α-helix structure with the representation of its hydrogen bonds.* ***Right:*** *a parallel plot of a β-plated sheet with the representation of its hydrogen bonds.*[11]

The tertiary structure refers to the folded polypeptide chain and represents the overall topology of the spatial arrangement of the amino acids along the polypeptide chain. The folding comes from the joining of the secondary structure, giving place to a compact globular molecule via interactions such as hydrogen bods, disulphide bridges, electrostatic interactions, and Van der Waals forces. For proteins longer than 150 amino acid units, the tertiary structure may be organized around more than one domain, which are structural units within the tertiary structure.[10]

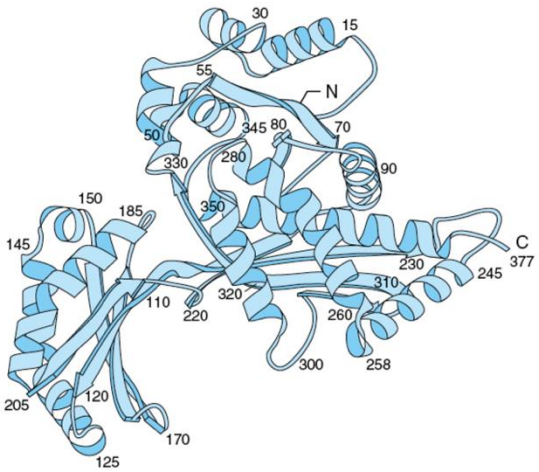

Figure 5*. Example of a protein tertiary structure, which shows two domains of a subunit of a dimeric protein.*

Finally, many proteins develop a higher organization degree and are made up of several protein monomers (which have their own primary, secondary and tertiary structures). This arrangement of subunits, leads to a functional complex known as the quaternary structure.[12]

Solid Phase Peptide Synthesis

Solid phase peptide synthesis (SPPS) was introduced by Merrifield in 1963. Since then, the chemistry related with this technique has developed dramatically, with improvements in the resins, protecting groups and methods of coupling and deprotection used during the synthesis. However, the basic synthetic tactics remain almost the same as those outlined by R.B. Merrifield more than five decades ago.[13]

The solid support used in this technique must be insoluble and should bear a linker with an appropriate functional group at which the first amino acid is attached. The stepwise SPPS usually proceeds in the *C* → *N* direction, so the linker must incorporate a functional group that reacts with the *C*-terminus of the first amino acid, conveniently protected at its *N*-terminus. Therefore, the synthesis proceeds by selective removal of the temporally amine protecting group of the first amino acid, followed by the coupling of the second, properly protected, amino acid. The coupling cycle continues until the peptide sequence has the desired length.[14]

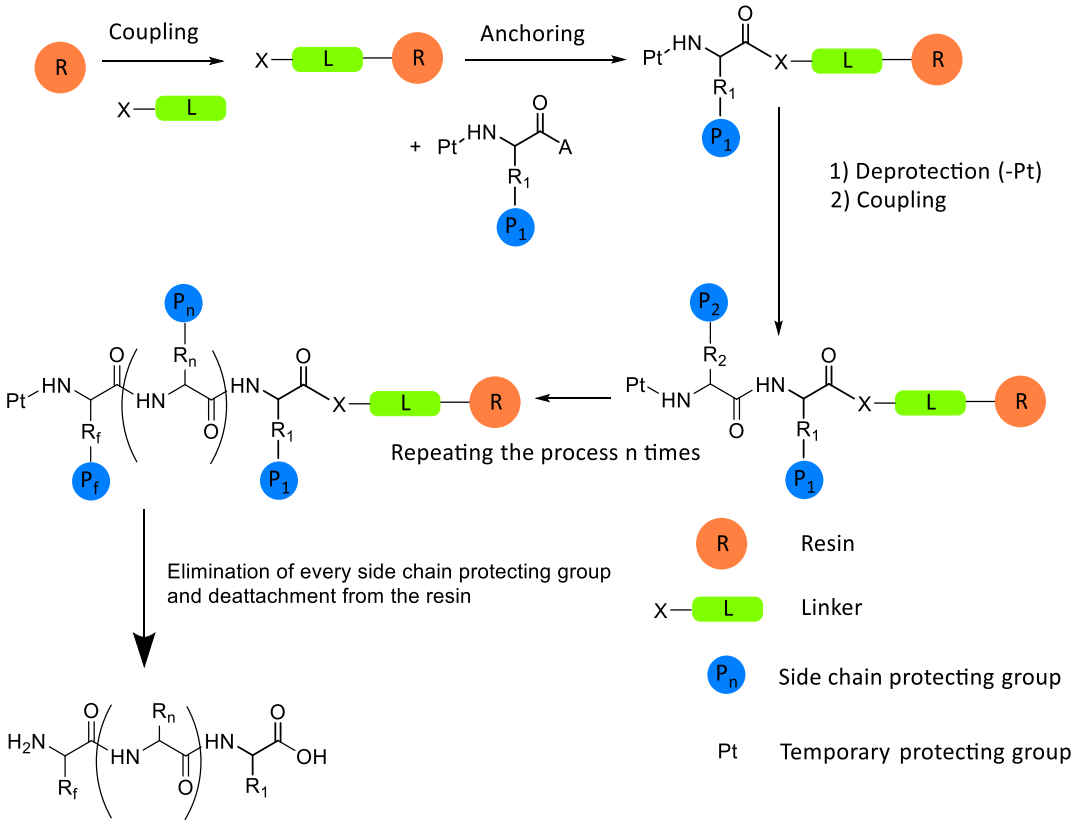

***Scheme 1**. Representation of the Solid Phase Peptide Synthesis steps.*

In peptide chemistry, a crucial issue for the synthesis of these polyfunctional molecules is the protection of their functional groups, since peptides can contain up to eight distinct functional groups in addition to indole and imidazole rings, which should

be also protected.[15] Therefore there are two main methods for peptide synthesis, which are classified depending on the protecting strategy used: Boc/Bn or Fmoc/*t*-Bu.

The Boc/Bn methodology uses *tert*-butylcarbonyl (Boc) as protecting group for the α-amino functionality of amino acids. The most common removal conditions for Boc are 25-50% TFA in DCM. Meanwhile, benzyl (Bn) group protects side chains of the amino acids, and it is generally removed with hydrofluoric acid, which is extremely dangerous.

On the other side, the Fmoc/*t*-Bu methodology uses 9-fluorenylmethoxycarbonyl (Fmoc) to protect the α-amino group and mild bases, mainly secondary amines such as piperidine in DMF, remove it. The *t*-Bu group protects the side chains and its removal is performed with TFA in the final step when the bond between the peptide and the solid support is also cleaved.[15]

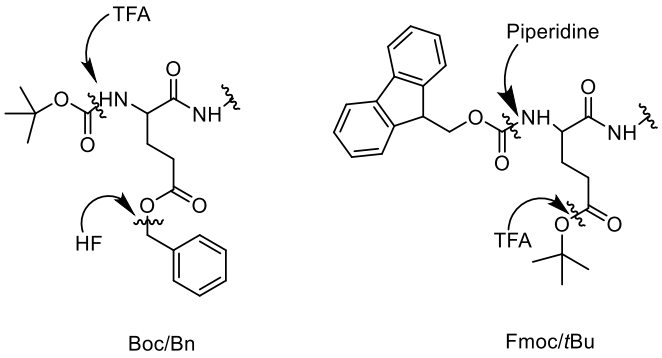

Figure 6. *Cleavage of protecting groups from the different strategies in SPPS.*

The key step in the peptide synthesis is the coupling between two amino acids, which involves the attack by the amino group of one residue at the carbonyl carbon of the carboxyl group, which has to be activated by the introduction of an electron withdrawing group.[16] Nowadays, there are four main ways to perform the activation:

a) Carbodiimides: they are one of the most widespread activating agents. Their main limitation is that they can produce dehydration of Asn and Gln residues, which can be avoided by the addition of HOBt to the reaction mixture. *N,N´*-dicyclohexyl derivative (DCC) is the most used carboiimide.[14]

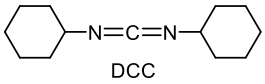

b) Mixed Carbonic Anhydrides: they are formed by reaction of an α-*N*-protected amino acid with alkyl chloroformates. The major advantages of this method are its simplicity and the high yields and purity of peptides obtained. However, a major drawback is racemization due to the highly activation of the carboxyl carbonyl that could lead to the oxazolone formation.[13]

c) Active Esters: they are generally formed by adding a trapping agent into a mixture of an α-*N* protected amino acid and DCC; therefore they may be considered somewhat into the carbodiimide method. Their major advantage is the formation of highly reactive amino acid esters which are capable of rapidly react with the amine of the other residue. The most common reagent is HOBt.[13]

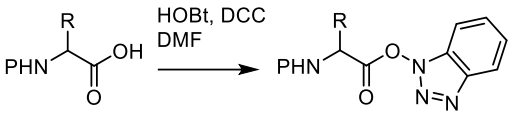

Figure 7. *Formation of an activated ester using HOBt.*

d) Phosphonium, aminium, and uronium salts: this method is the most important one, since it provides high purity of peptides and excellent yields even in difficult couplings. Uronium salts have been shown the ability to form activated species even in polar solvents, which has application in automated SPPS.[13]

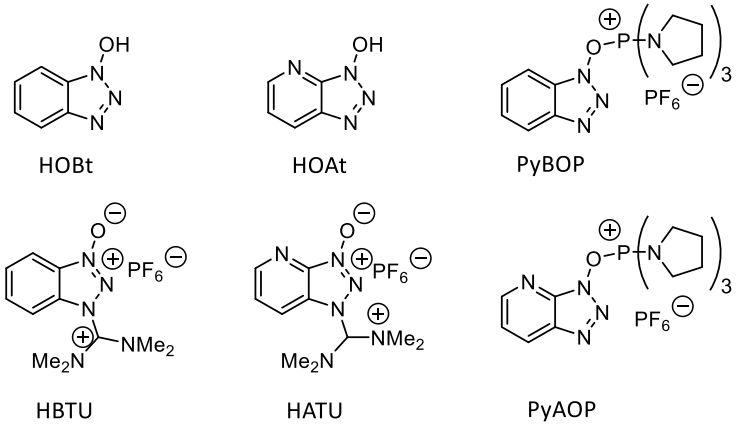

Figure 8*. Most common phosphonium salts used as activating agents in SPPS*

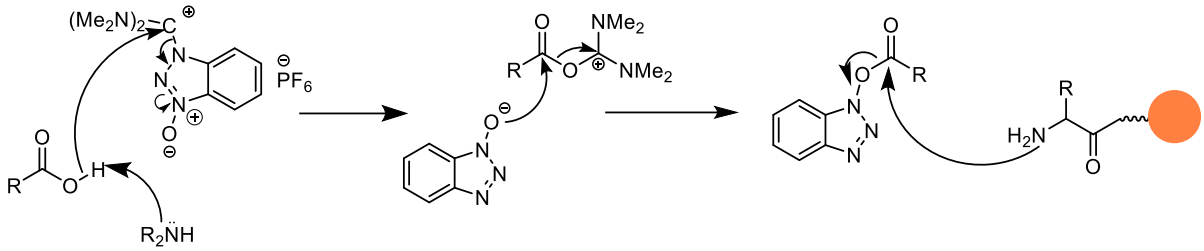

Figure 9. *Formation in situ of an activated ester and coupling with the polypeptide.*

LANTHANIDE IONS AND THEIR BEHAVIOR IN COORDINATION CHEMISTRY

Lanthanides are those elements that follow lanthanum in the periodic table, from cerium to lutetium, making a homogenous group with a total of fourteen elements. They show a high uniformity in their chemical properties, behaving as electropositive metals that have a strong preference to the trivalent oxidation state.

The reason for the occurrence of the trivalent oxidation state in the lanthanide ions, Ln(III), is given by the relative energies of the electronic orbitals 4*f*, 5*d*, 6*p* and 5*s* along the fourteen different elements, from Z=57 to 71 (Table 1). The enthalpy balance of the atomization, ionization and hydration enthalpies determines that the trivalent state of the lanthanide ions is the most stable one occurring in aqueous solution across the whole lanthanide series. The hydration enthalpy increases along the series since the ionic radius decreases from La^{3+} to Lu^{3+}. However, the redox potentials keep quite similar throughout the series, which at the beginning and the end of the series take the

values Eº(La^{3+}/La) = -2.38 V and Eº(Lu^{3+}/Lu) = -2.30 V. Thus, the increasing hydration enthalpies are compensated by higher ionization potentials on advancing along the series. The exception comes from the Ce^{4+}, which is the only tetrapositive element with interest in aqueous solution. In acid solution it behaves as a stronger oxidant than chlorine, presenting the ability to remain in solution for long periods of time.[17,18] The stabilization of the divalent oxidation states of Eu and Yb is related to the half-filled ($4f^7$) and complete ($4f^{14}$) occupation of the 4f shell in Eu^{2+} and Yb^{2+}, respectively (Table 1).

Table 1. *Electronic configuration of the lanthanide ions and their respective cations.*

Atomic number	Name	Symbol	Atom	M^{2+}	M^{3+}	M^{4+}
57	Lanthanum	La	$5d^16s^2$	$5d^1$	[Xe]	-
58	Cerium	Ce	$4f^15d^16s^2$	$4f^2$	$4f^1$	[Xe]
59	Praseodymium	Pr	$4f^36s^2$	$4f^3$	$4f^2$	$4f^1$
60	Neodymium	Nd	$4f^46s^2$	$4f^4$	$4f^3$	$4f^2$
61	Promethium	Pm	$4f^56s^2$	$4f^5$	$4f^4$	-
62	Samarium	Sm	$4f^66s^2$	$4f^6$	$4f^5$	-
63	Europium	Eu	$4f^76s^2$	$4f^7$	$4f^6$	-
64	Gadolinium	Gd	$4f^75d^16s^2$	$4f^75d^1$	$4f^7$	-
65	Terbium	Tb	$4f^96s^2$	$4f^9$	$4f^8$	$4f^7$
66	Dysprosium	Dy	$4f^{10}6s^2$	$4f^{10}$	$4f^9$	$4f^8$
67	Holmium	Ho	$4f^{11}6s^2$	$4f^{11}$	$4f^{10}$	-
68	Erbium	Er	$4f^{12}6s^2$	$4f^{12}$	$4f^{11}$	-
69	Thulium	Tm	$4f^{13}6s^2$	$4f^{13}$	$4f^{12}$	-
70	Ytterbium	Yb	$4f^{14}6s^2$	$4f^{14}$	$4f^{13}$	-
71	Lutetium	Lu	$4f^{14}5d^16s^2$	-	$4f^{14}$	-

The ionic radii of the Ln^{3+} ions decrease slightly with the increase in atomic number. Given their large ionic radii, the lanthanide ions generally form complexes with high coordination number and different coordination polyhedra. Their coordination number (CN) is usually 8 or 9, with some exceptions, while the coordination geometry is dictated by the topology and the steric effects caused by the ligands. Table 2 lists the effective ionic radii for the most common CNs of the lanthanide ions.[18,19]

Table 2. *Effective ionic radii for the Ln(III) ions.*

Cation	CN 6	CN 8	CN 9	Cation	CN 6	CN 8	CN 9
La^{3+}	1.032	1.160	1.216	Tb^{3+}	0.923	1.040	1.095
Ce^{3+}	1.01	1.143	1.196	Dy^{3+}	0.912	1.027	1.083
Pr^{3+}	0.99	1.126	1.179	Ho^{3+}	0.901	1.015	1.072
Nd^{3+}	0.983	1.109	1.163	Er^{3+}	0.890	1.004	1.062
Pm^{3+}	0.97	1.093	1.144	Tm^{3+}	0.880	0.994	1.052
Sm^{3+}	0.958	1.079	1.132	Yb^{3+}	0.868	0.985	1.042
Eu^{3+}	0.947	1.066	1.120	Lu^{3+}	0.861	0.977	1.032
Gd^{3+}	0.938	1.053	1.107				

The Ln(III) ions are hard Lewis acids according to Pearson's classification of hard and soft acids and bases. As a result, the Ln^{3+} ions have a strong preference to form thermodynamically stable complexes with ligands having hard donor atoms such as oxygen and nitrogen, particularly if they hold negative charges. In particular, the lanthanide ions form stable complexes with polyamino polycarboxylate-type ligands containing 8 or 9 potential donor atoms. For instance, the macrocycle 1,4,7,10-tetraazacyclododecane-1,4,7,10-tetraacetic acid (DOTA, Figure 10) forms thermodynamically stable complexes with Ln(III) ions that also present very slow dissociation kinetics.[20] The coordination chemistry of DOTA and DOTA-derivatives with the Ln^{3+} ions has been extensively investigated, in part because of the application of the $[Gd(DOTA)]^-$ complex in clinical practice as a contrast agent in magnetic resonance imaging (MRI). DOTA-tetraamide derivatives such as DOTAM (Figure 10) were found to form complexes far less stable than DOTA, but they show slower dissociation kinetics.[21] Complexes of Eu^{3+} and Tb^{3+} with DOTA derivatives have been extensively investigated as luminescent probes.[22]

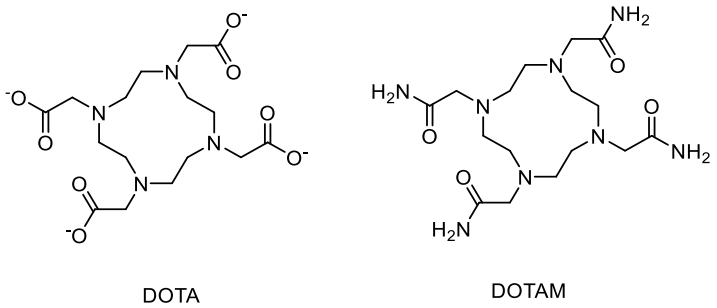

Figure 10. *Structure of the DOTA and DOTAM ligands.*

The complexes of DOTA and DOTAM with the lanthanide ions are eight-coordinated by the ligand, with a water molecule completing coordination number nine. The presence of this coordinated water molecule is essential for application of the Gd^{3+} complex as an MRI contrast agent, but it is detrimental for the luminescence efficiency of Eu^{3+} and Tb^{3+} derivatives.

It should be mentioned that the mechanisms for the formation of DOTA and DOTAM complexes are different. While $[Ln(DOTAM)]^{3+}$ complexes form in a direct reaction between the deprotonated DOTAM and the Ln^{3+} ion, in the case of DOTA, a diprotonated intermediate is formed by the coordination of the Ln^{3+} with the acetate groups of the deprotonated ligand. This intermediate experiences proton transfer from the nitrogen atoms of the macrocycle to the donor atoms of the acetate groups, so that the metal enters into the macrocyclic cage.[23]

LUMINESCENCE

GENERAL CONCEPTS

Fluorescence refers to a well-known phenomenon in which a photon is emitted from an excited molecule that relaxes to its ground state. Usually, fluorescence occurs if the transition takes place without change in the spin of the system, and thus generally involves emission from the first excited singlet state to the ground singlet state ($S_1 \rightarrow S_0$). Transitions implying a change in the spin of the system are the origin of phosphorescence, for instance arising from emission from the first excited triplet state to the ground singlet state ($T_1 \rightarrow S_0$). The 0–0 transition, which involves the lowest-energy vibrational states of the ground and excited levels, should present the same energy in the absorption and fluorescence spectra. However, the fluorescence spectrum is shifted to longer wavelengths (lower energy) with respect to the absorption spectrum due to the energy loss in the excited state by vibrational relaxation. The different processes that occur when a molecule absorbs a photon and reaches an exited state are represented in a Jablonski Diagram provided in Figure 11.[24]

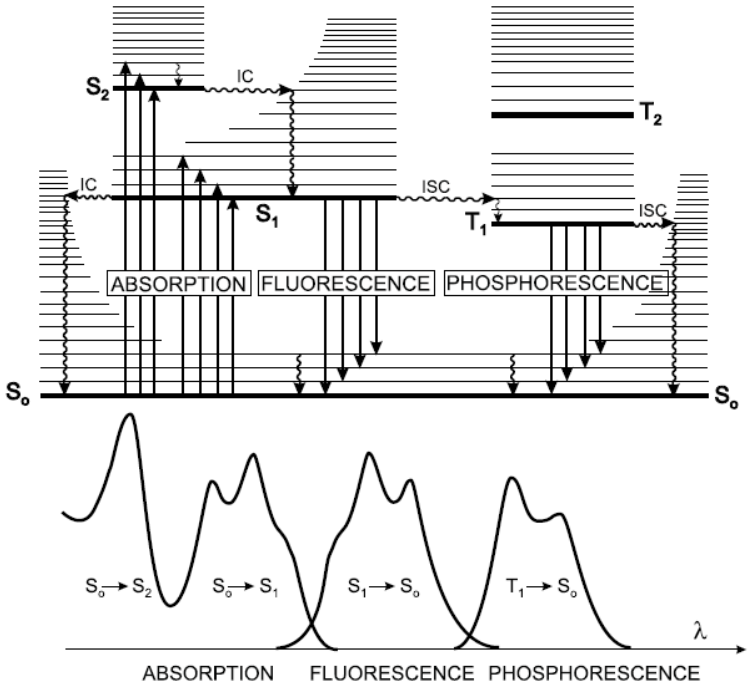

***Figure 11**. Jablonski diagram where the different processes that occur when a molecule absorbs a photon and jumps to an excited state. The molecule could also return to its ground state through a non-radiative relaxation process. ISC: Intersystem crossing; IC: Internal conversion.*[24]

The interactions of the molecule and its environment determine to a great extent several factors such as the lifetime of the excited state and the quantum yield of the emission process. The quantum yield refers to the ratio of emitted and excited photons, and is generally expressed as a percentage.

Fluorescence probes have gained increasing attention in different research areas due to their specificity and sensitivity, along with the possibility to obtain spatial and time information with good resolution. Indeed, fluorescent probes allowed the development of techniques in biology that resulted in a dramatic improvement in the

comprehension of the structures and different phenomena of biomolecules. The design of fluorescent sensors has therefore a high demand for several clinical and biochemical applications.

Lanthanide Luminescent Complexes

Most of the lanthanide ions are found in their trivalent form (Ln^{+3}), unlike transition metal elements, which possess a huge variety of oxidation states. The optical properties of Ln^{+3} ions present some relevant features associated to a great variety of electronic levels due to their $[Xe]4f^n$ configurations. Each level is defined by three quantum numbers, *S*, *L*, and *J*, within the framework of the Russel-Saunders spin-orbit coupling scheme. The energy of each of them is well defined since the 4f orbitals are shielded by the filled $5p^6 6s^2$ subshells. Moreover, the energies of f-f transitions are not very affected by the chemical environment of the ion, due to the core nature of the 4f orbitals. Depending on the particular Ln^{3+} ion the 4f-4f transitions may be observed in the visible and near-infrared (NIR) regions, and they are easily recognizable because they are quite sharp (see Figure 12). The major advantage of these f-f transitions is that they are parity forbidden, which results in lifetimes of the excited states that are generally longer than in other ions and organic fluorophores. This makes the lanthanide ions quite useful in time-resolved detection and luminescence microscopy.[25]

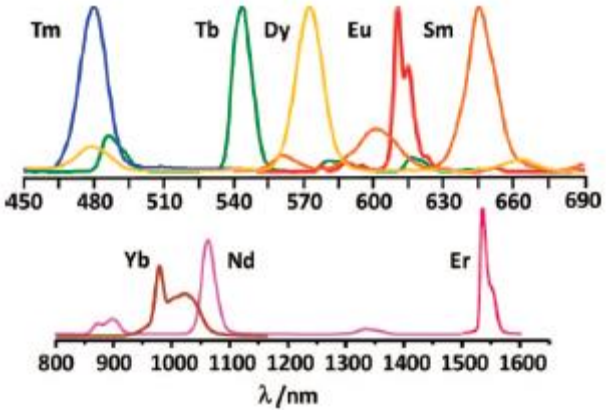

Figure 12. *Luminescence spectra of some lanthanide tris(β-diketonates).*[25]

The major drawback of the lanthanide ions is that direct excitation of the 4f excited states is very inefficient, a problem related to the electric dipole selection rules, which forbid such transitions.[26] Therefore, another approach has to be taken in order to improve the emission intensity. This is rather efficiently achieved by using the so called antenna effect, which relies on an indirect excitation as follows (Figure 13):

1. The light is absorbed by an organic chromophore in the vicinity of the Ln^{+3} ion.

2. Then the energy is transferred to the metal ion, which is excited to one or several excited states.

3. Fluorescence emission is produced by relaxation of the metal that returns to its ground state.

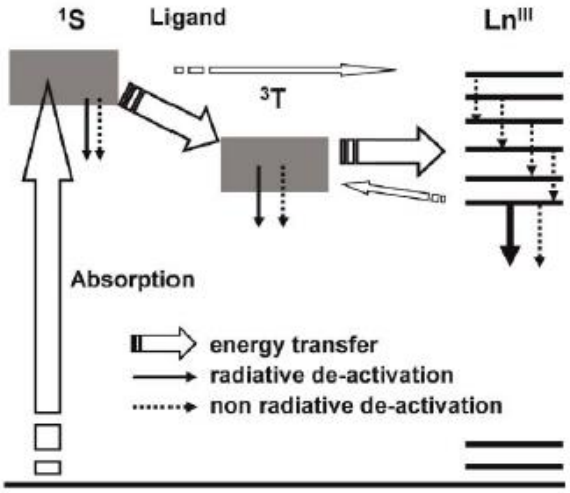

Figure 13. *Diagram showing the main energy flow paths during indirect excitation of lanthanide luminescence via the surroundings (ligands).*[16]

A lanthanide-based luminescent sensor should provide a selective change of the luminescent signal that is related to the concentration of the analyte. Ideally, the luminescent response should be such that the emission intensity is enhanced in the presence of the analyte. The modulation of Ln^{3+} luminescence can be achieved through three different mechanisms (see Figure 14):

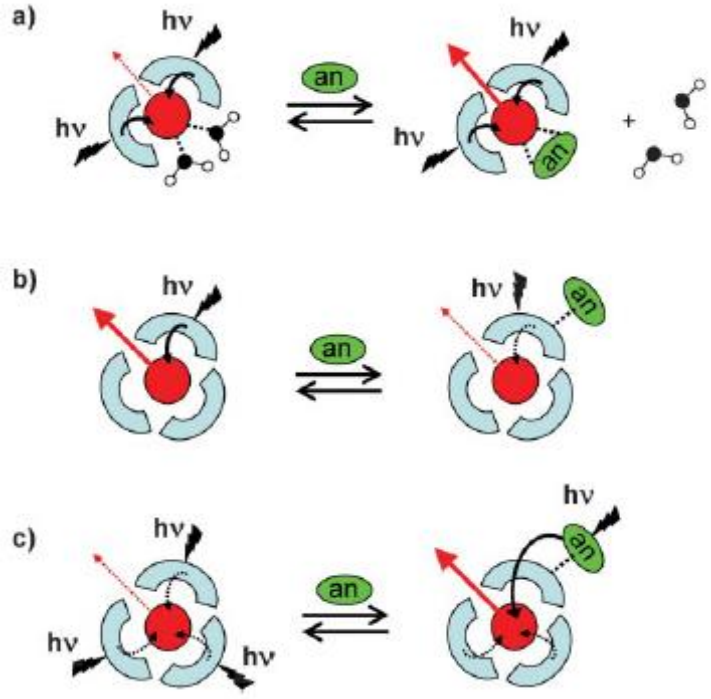

Figure 14. *Representation of the different mechanisms operating in the modulation of lanthanide emission by reversible binding of an analyte.*

a) Acting directly on the Ln^{+3} ion, which provides a signal that depends on the chemical environment. For example, water molecules in the coordination sphere are well known to quench the emission of Ln^{3+} ions. Therefore, the replacement of coordinated water molecules by the analyte usually provokes an enhancement of the luminescent signal.

b) Another approach consists in modifying the photophysical properties of the ligand when the analyte is attached, for instance intra- or inter-molecular quenching of the ligand-centered singlet or triplet states.

c) Lastly, the analyte may also play the role of acting as a sensitizer of the Ln^{+3} ion or even as a quencher.

Background

The use of lanthanide luminescence is an attractive strategy for the detection and monitoring of biological activity in cells, since luminescence provides a reliable, sensitive and non-invasive technique for the following of such processes. Moreover, the long emission lifetimes of the Ln^{3+} ions allow time-resolved measurements that can be used to eliminate interferences from the luminescence of biomolecules.[22]

In 2012, the group of M. E. Vázquez designed a Eu^{3+} peptide complex whose luminescence signal is modulated by the phosphorylation state of a serine residue incorporated in the peptide sequence, in such way that the probe can monitor the enzymatic activity of both protein kinase C (PKC) and alkaline phosphatase (AP). The heptadentate DO3A (1,4,7,10-tetraazacyclododecane-1,4,7-triacetic acid) macrocyclic ligand does not satisfy all the coordination sites of the metal ion, which contains one coordinated water molecule. However, an external antenna can fill this position providing a highly emissive complex. However, when the serine residue is phosphorylated by PKC, the phosphate group coordinates the metal and displaces the antenna from the coordination sphere, promoting a decrease of the emission intensity. Addition of AP over the phosphorylated probe in the presence of the external antenna restores the emission of the Eu(III) complex due to the dephosphorilation of the serine residue (Figure 15).[27,28]

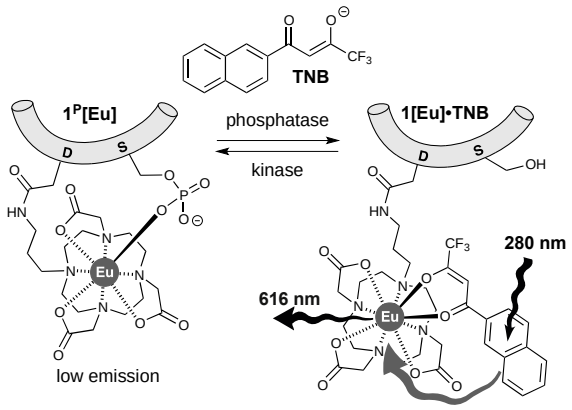

***Figure 15**. Proposed mechanism for the generation of a luminescence signal with the added coordination antenna to excite the lanthanide ion.*[28]

A more recent example published in 2015, showed that terbium complexes are useful for monitoring the activity of NAD(P)H-dependent enzymes. In this case, the authors reported a terbium (III) complex with a 1,4,7,10-tetraazacyclododecane functionalized with amide ligands and an azaxanthone antenna. The resulting luminescent complex has a +3 net charge that can electrostatically interact with NADH or NADPH molecules that are negatively charged (-2 and -4, respectively). This interaction promotes the quenching of the luminescence of the complex. Therefore, this system can be applied for monitoring the activity of NAD(P)H dependent enzymes, such as lactate dehydrogenase. The addition of this enzyme over the Tb(III)complex-NADH mixture in presence of pyruvate, promotes the reduction of pyruvate to lactate and

transforms NADH in NAD+, destroying its interaction with the Tb(III) complex and therefore recovering its luminescence.[29]

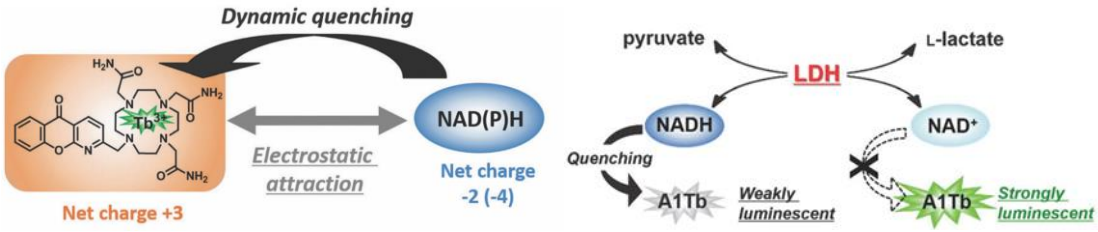

***Figure 16. Left**: Scheme of the interaction of a Tb(III) complex with NAD(P)H. **Right:** representation of the lactate dehydrogenase activity detection assay.*[29]

Objective

The aim of this work is to develop an optical sensor, based on the luminescence of lanthanide ions, for the detection of nitro-oxidative stress in cells. The design relies on the incorporation of a Ln^{3+} chelate in a peptide sequence derived from α-synuclein, known to be nitrated *in vitro* and *in vivo*, allowing to use the generated 3-nitrotyrosine chromophore as lanthanide sensitizer.

The ligands chosen for this project were designed to provide coordinatively unsaturated Ln^{3+} complexes, so that water molecules are expected to complete the metal coordination environment in aqueous solution. These water molecules should quench the excited state of the Ln^{3+} ion through vibrational deactivation. The change of the pK_a of the hydroxyl group with respect to tyrosine upon nitration of the peptide (≈7 and ≈10 respectively) may result in a partial deprotonation of the phenol group at physiological pH. We hope that this will trigger the coordination of the phenolate group to the Ln^{3+} ion, causing the displacement of the coordinated water molecules. This would generate a complex with higher luminescence promoted both by the shorter distance between the antenna and the metallic centre, and by the displacement of water molecules from the inner-coordination sphere of the metal ion. Thus, in this work we wanted to perform some preliminary work towards the aim of developing a sensor of oxidative stress (Figure 17). More specifically, this work aimed at:

1. Synthesis of two peptide sequences, one of them containing a tyrosine residue and the other a 3-nitrotyrosine residue.
2. Synthesis of the macrocyclic ligand modified with an amine group, so that it can be coupled to the peptide.
3. Coupling between the lanthanide chelate and both peptides.

Subsequent studies will complete this work by studying the coordination of the lanthanide ion by the modified peptides, studying the luminescent properties of both lanthanide-peptide complexes, and the assessment of the potential use of 3-nitrotyrosine as lanthanide sensitizer.

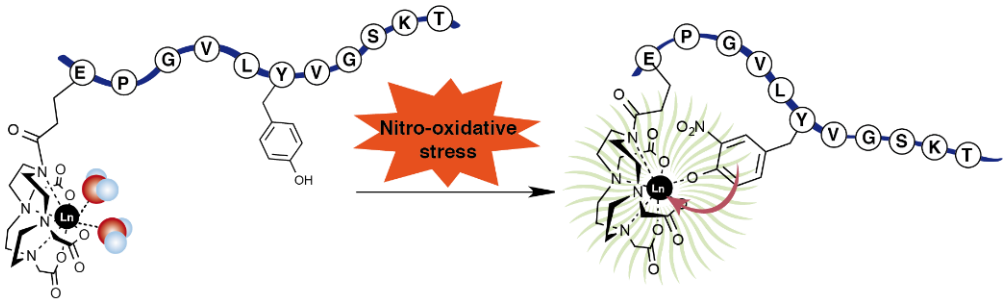

***Figure 17**. Scheme of the proposed sensor and its mechanism for giving a luminescent response upon oxidative stress.*

While being a scientific work, it should be pointed out that the work carried out during this Final Degree Project involves also a strong pedagogical component. The work carried out in this project contributed to strengthen and develop different skills and competences related to the bachelor degree in chemistry. Among the competences developed during this work are:

Objective

Learning outcomes	Degree competences
To understand the concepts, methods and results of the major areas of chemistry.	A1, A14, B3, C2, C8
To be able to interpret data, information and relevant results, obtaining conclusions and make thoughtful reports about scientific problems. To work, learn and research resources independently.	A16, A24, B2, B4, C1, C2, C3, C4, C6
To be able to apply theoretical knowledge along with practical skills that have been acquired during the degree and proposed solutions related to the academic or professional field.	B2, B3, B4, B5, B6, C4, C6

Results & Discussion

PEPTIDES DESIGN AND SYNTHESIS

PEPTIDE DESIGN

The design of the sensor was accomplished by selecting sequences of α-synuclein that have been found nitrated both *in vitro* and *in vivo*.[30] Specifically, we sought to modify the ^{36}GVLYVGSKT^{44} fragment by adding: 1) a Pro residue at its *N*-terminus, since Pro-Gly is a ß-turn inducing sequence that could preorganize the peptide chain to favor the complexation of the antenna, and 2) a Glu residue to which the metal complex will be conjugated in its side chain. Therefore, based in this sequence, we designed two peptides (Figure 18) differing only in the tyrosine residue. In the case of P1 the tyrosine residue is not modified and in the case of P2 this residue is nitrated (3-nitrotyrosine).

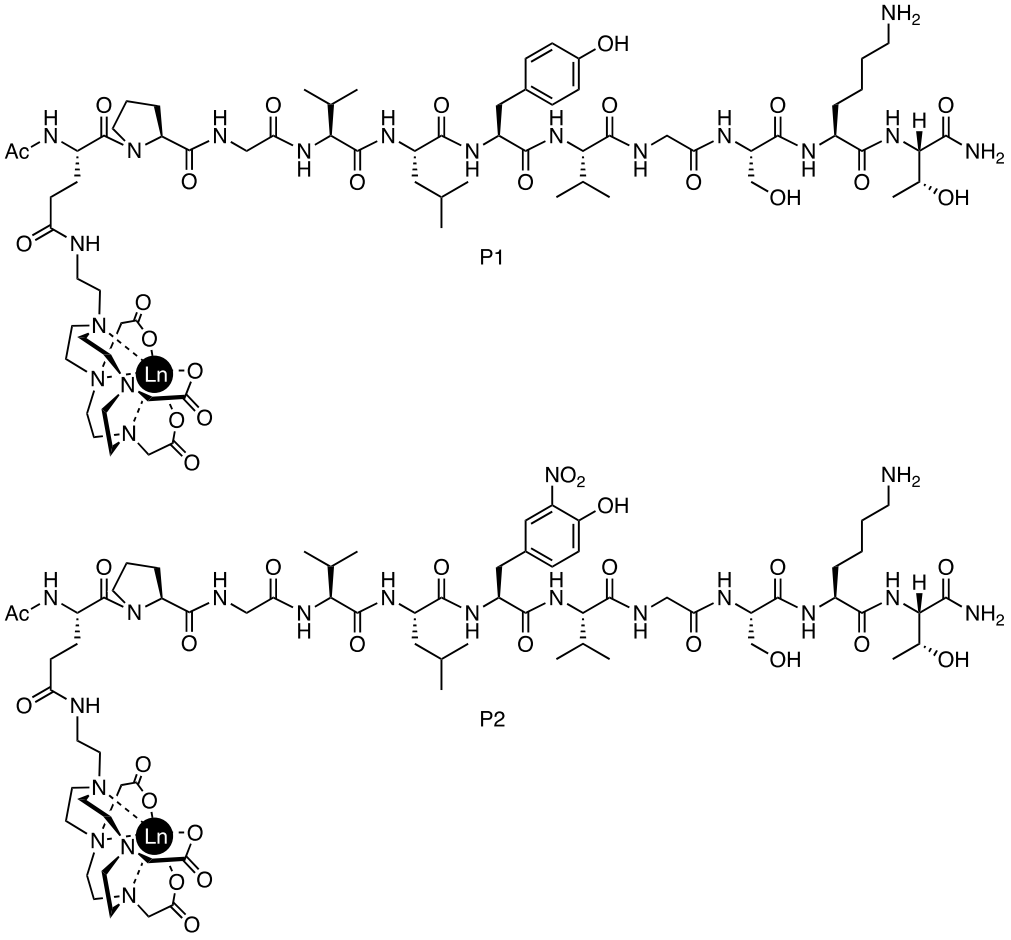

***Figure 18**. Structure of the designed P1 and P2 peptides.*

As for the lanthanide binding unit, we have chosen a chelator based on a DO3A scaffold (Figure 18, DO3A = 1,4,7,10-tetraazacyclododecane-1,4,7-triacetic acid). The heptadentate DO3A unit is known to form rather stable complexes with the Ln^{3+} ions, combined with relatively slow dissociation kinetics. Furthermore, the [Ln(DO3A)] complex is coordinatively unsaturated, and contains two water molecules bound to the metal center. These complexes are also known to bind reversibly different anions, and

therefore the [Ln(DO3A)] motif appears to be a good choice for the envisaged application.

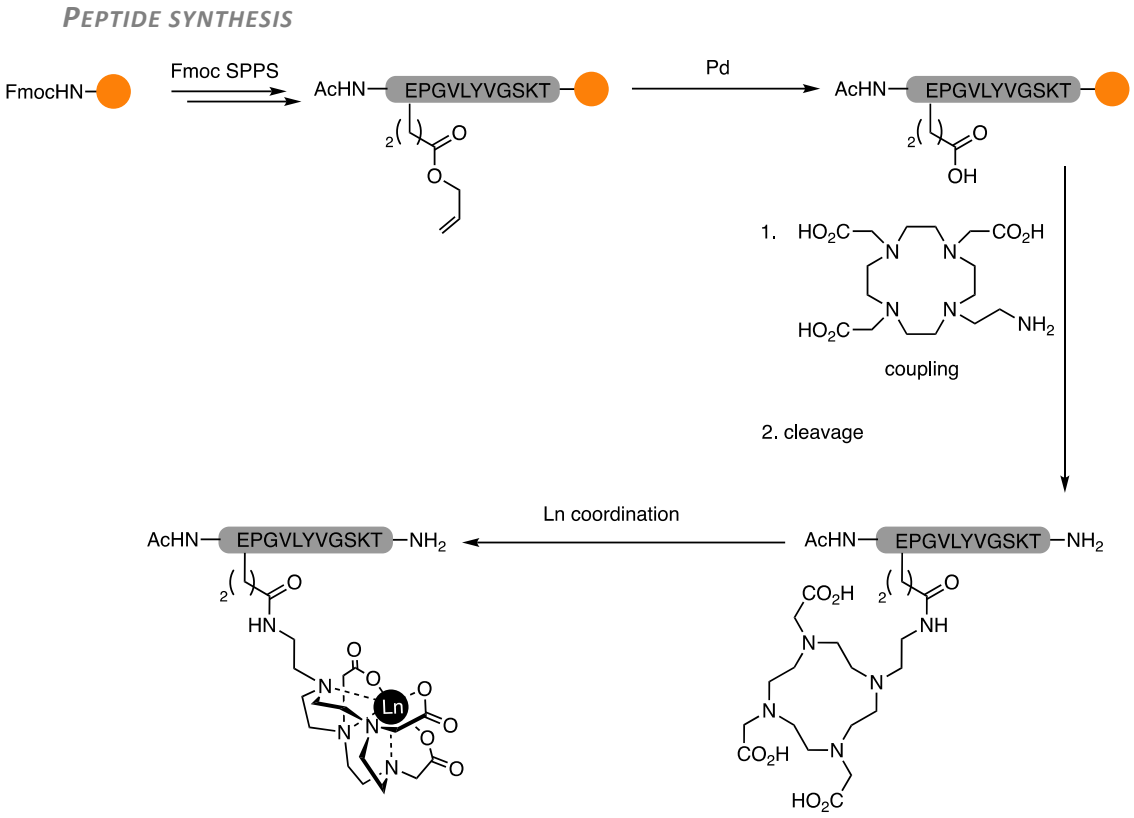

Scheme 2. *General synthetic strategy for P1 and P2 synthesis (in this case only P1 is shown).*

The peptides were synthesized using standard solid phase peptide synthesis protocols following the the Fmoc/*t*-Bu strategy. All the couplings were efficiently performed and there was no need of recoupling any amino acid (Scheme 2).

From the chosen sequence, residues Thr, Ser and Tyr all have their side chain –OH group protected with *tert*-butyl units, while the side chain of Lys has its functional group protected with a Boc group. All of them can be efficiently removed by TFA, which also cleaves the peptide chain from the resin. The Glu residue has its side chain protected with an allyl group, which is removed through palladium catalysis.

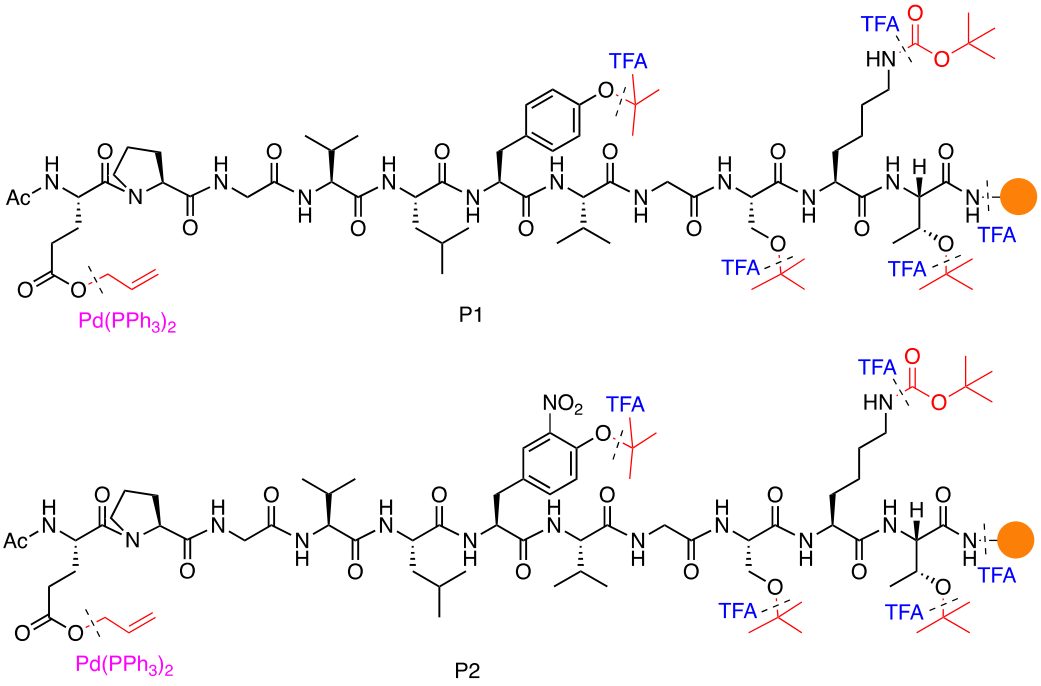

***Figure 19**. Structure of the designed P1 and P2 peptides attached to the solid support. The protecting groups of the side chains are highlighted in red, along with the reagents used in order to remove them and to cleave the peptides from the solid support.*

Once all couplings were performed, and before the removal of the Allyl group, the peptides were cleaved from the resin and analyzed by reverse phase HPLC-MS in order to check whether the peptide synthesis was successful. For peptide P1, the HPLC chromatogram (Figure 20) presents a mayor peak at t_r = 16.4 min that was identified by ESI-MS as the desired product (*m/z* = 1230.5, Figure 20).

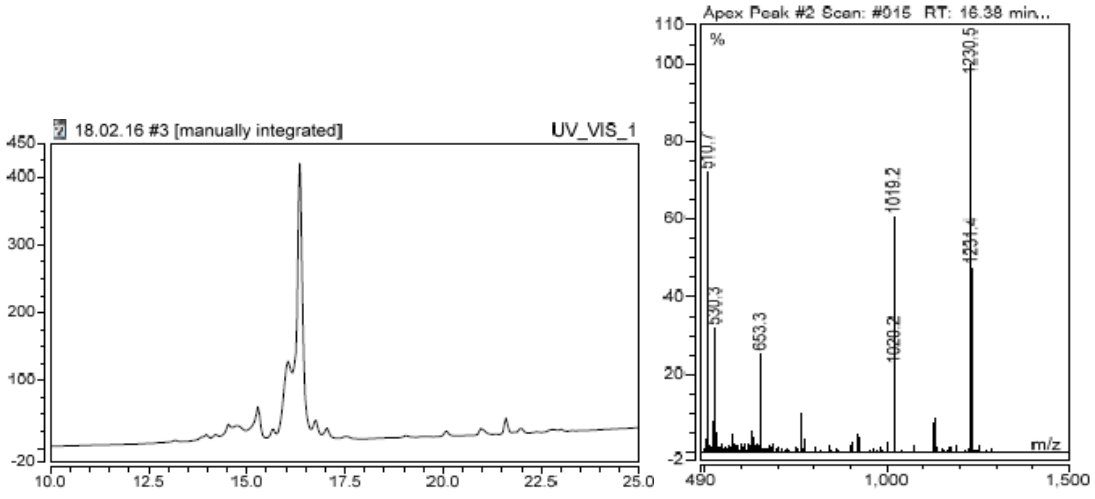

***Figure 20.** HPLC chromatogram of the reaction crude in which the peak at t_r = 16.4 min corresponds to P1. ESI-MS of the HPLC peak at t_r = 16.4 min.*

In the case of P2, a mayor peak in the HPLC chromatogram (Figure 21) at t_r = 17.4 min was identified as the expected nitrated peptide, as confirmed by the presence of a major signal at *m/z* = 1275.4 corresponding to the desired peptide protected with the

allyl group. Hence, after corroborating the formation of both P1 and P2 peptides the following step (removal of the allyl group) was performed.

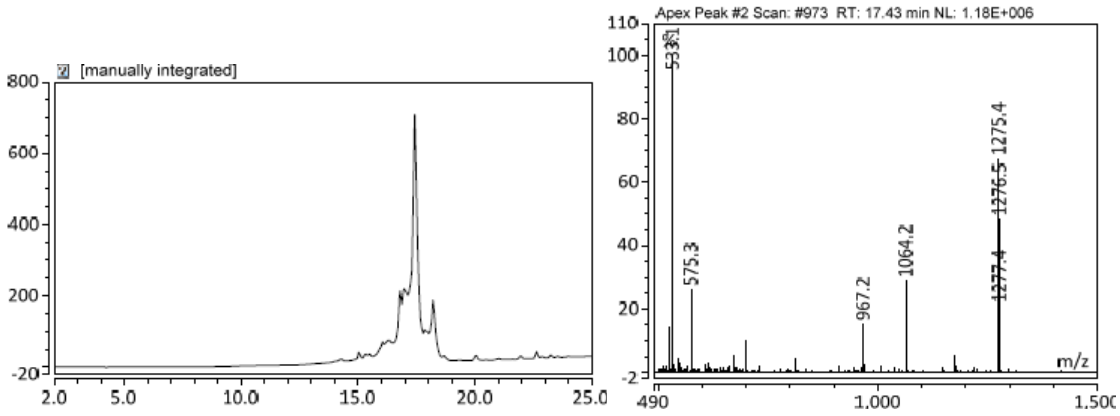

Figure 21. *HPLC chromatogram of the reaction crude in which the peak at t_r = 17.4 min corresponds to P2. ESI-MS of the HPLC peak at t_r = 17.4 min.*

ALLYL GROUP DEPROTECTION

Since the coupling of the DO3A fragment requires the condensation of the amine group present in the macrocycle and the carboxylic acid of the Glu side chain, while the peptide is attached to the solid support, we chose an allyl unit as orthogonal protecting group for the Glu side chain. This group can be selectively removed by catalytic treatment with Pd affording the desired carboxylic acid without affecting any of the other amino acid protecting groups. The mechanism is described below (Scheme3); the final nucleophilic attack was carried out using triphenylsilane and *N*-methylmorpholine.

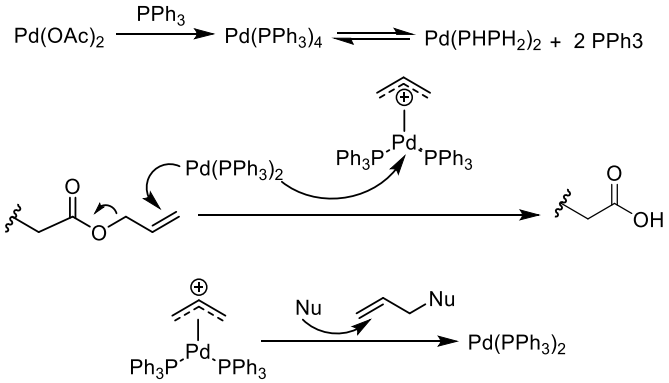

Scheme 3. *Mechanism for the deprotection of the allyl group.*

The analyses by HPLC-MS of a small portion of each resin confirmed the deprotection of the Glu side chain, obtaining a peak at t_r = 11,4 min corresponding to P1 (*m/z* = 1190.6, Figure 22) and a peak at t_r = 12.3 min corresponding to the nitrated peptide P2 (*m/z* = 1235.7, Figure 23).

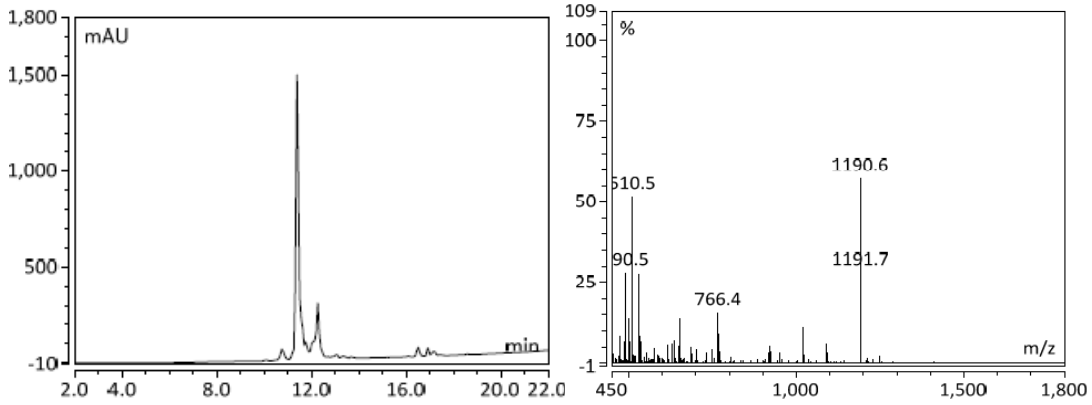

Figure 22. *HPLC chromatogram of the reaction crude in which the peak at t_r = 11,4 min corresponds to P1 without the allyl group. ESI-MS of the HPLC peak at t_r = 11,4 min.*

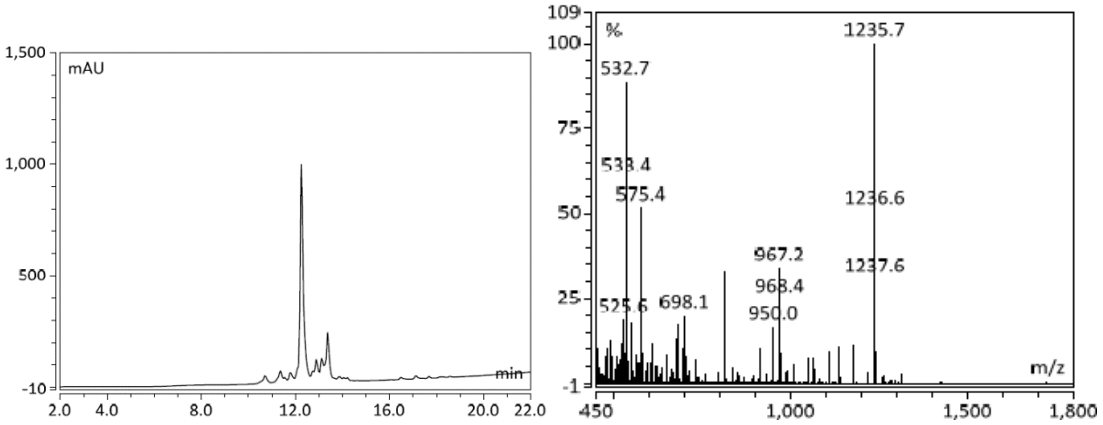

Figure 23. *HPLC chromatogram of the reaction crude in which the peak at t_r = 12.3 min corresponds to P2 without the allyl group. ESI-MS of the HPLC peak at t_r = 12.3 min.*

SYNTHESIS OF LIGAND L1

L1 was synthesized following the protocols described in literature (Scheme 4).[31] First, the commercially available DO3AtBu ligand was alkylated with *N*-Boc-2-bromoethylamine through a nucleophilic substitution of the bromine by the secondary amine of the ligand. The corresponding product was characterized by ESI-MS (658.48 m/z). The subsequent step was the deprotection of the carboxylic acid groups, along with the removal of the Boc protecting group of the amine, by treatment with TFA. The obtention of the desired product was confirmed by ESI-MS (390.23 m/z). The ^{1}H NMR spectrum recorded in D_2O solution presents broad signals in the range 2.5-4.5 ppm, a feature that is characteristic of DO3A derivatives. The ^{13}C NMR spectrum was more informative, showing two broad signals due to the carbonyl groups at 175.1 and 170.1 ppm, together with a sharper resonance at 174.4. This suggests a relatively high degree of rigidity of the macrocycle. The aliphatic region shows up to 13 signals, which points to a C_1 symmetry of the ligand in D_2O solution. The spectrum also shows two quadruplets

at 162.8 ppm ($^2J_{C-F}$ = 35.5 Hz) and 114.9 ppm ($^1J_{C-F}$ = 292 Hz) due to TFA, which indicates that the L1 ligand was isolated as the trifluoroacetate salt.

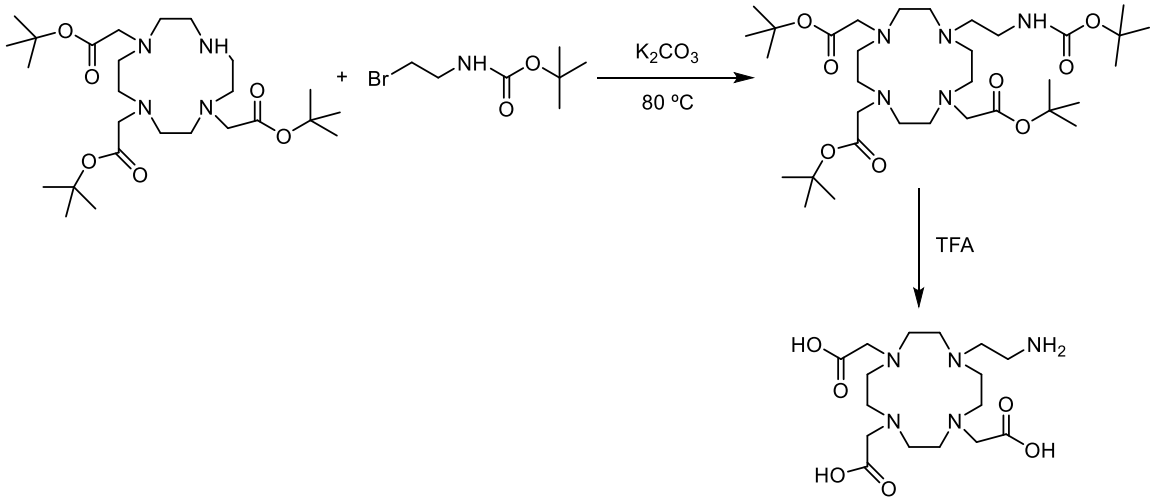

Scheme 4. *Synthetic route followed for the synthesis of ligand L1.*

COUPLING OF LIGAND L1 TO PEPTIDES P1 AND P2

The coupling of L1 to the deprotected carboxylic acid side chain of the Glu residue of both peptides P1 and P2 was carried out with the peptides still attached to the solid support. The method used for the coupling of the ligands was the activation of the carboxylic group by the *in situ* formation of the activated ester with HATU, which reacts with the amine group present in L1.

After performing the coupling, a small portion of each resin was analyzed by HPLC-MS (Figure 24). For P1 the HPLC chromatogram shows three peaks, in which the peak at t_r = 10.9 min was identified by ESI-MS as the desired peptide with L1 attached, the peak at t_r = 11.4 min was identified by ESI-MS as the unmodified peptide, and the peak at t_r = 12.3 min was identified by ESI-MS as the unmodified peptide in which the free carboxylic acid experienced an intramolecular condensation to form an unreactive lactam. The HPLC chromatogram obtained indicates that the desired peptide coupled to the DO3A unit was obtained as a minor product, with the unreacted peptide and that resulting from lactam formation giving more intense peaks.

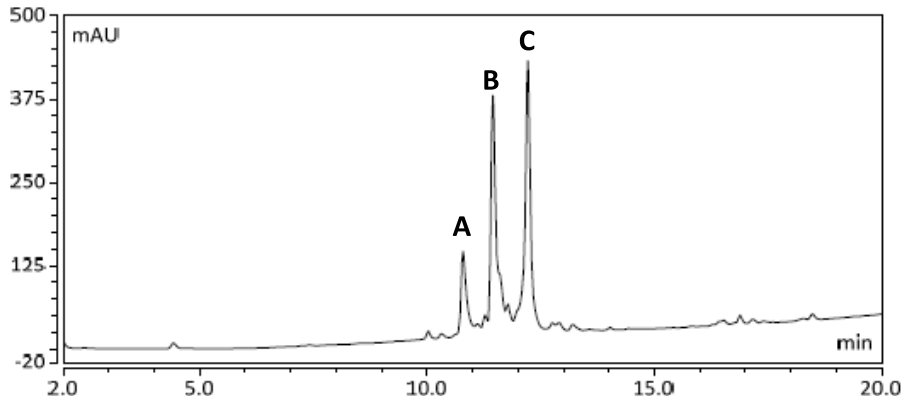

Peak	t_R (min)	MS (m/z)	Assignment
A	10.9	782.0 $[MH_2]^{2+}$	Product
B	11.4	1190.6 $[MH]^+$	P1
C	12.3	1172.5 $[MH]^+$	P1 (-H_2O)

Figure 24. *HPLC chromatogram of the coupling between L1 ligand and P1 with each peak analysed by mass spectrometry.*

In the case of P2 the HPLC chromatogram (figure 25) showed many peaks. However, despite this, the peak at t_r = 11.6 min could be identified by ESI-MS as the desired product and the peak at t_r = 12.3 min could be identified by ESI-MS as the unmodified peptide P2.

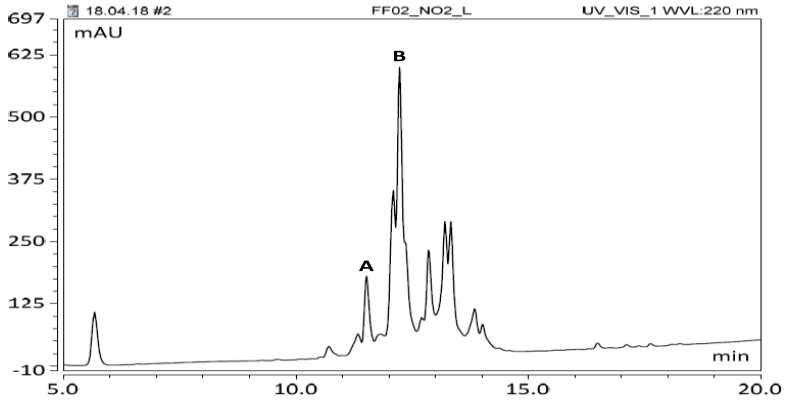

Peak	t_R	MS (m/z)	Assignment
A	11.6	804.5 $[MH_2]^{2+}$	Product
B	12.3	1235.4 $[MH]^+$	P2

Figure 25. *HPLC chromatogram of the coupling between P2 and L1 ligand with each peak analyzed by mass spectrometry.*

After analyzing the obtained results, the coupling was performed using the less reactive coupling agent HBTU, but the results obtained in these cases did not improved the ones just described for HATU.

As an alternative to improve the coupling of L1 to P1 and P2, we attempted to obtain the EuL1 complex, hoping that the complex could be more efficiently coupled to

the peptide. Thus, we reacted the L1 ligand with different Eu^{3+} salts ($EuCl_3$ and $Eu(OTf)_3$), using different bases to ensure the deprotonation of the carboxylate groups (Et_3N, K_2CO_3) and solvents (water and 2-propanol). The complexation reaction was followed by ESI-MS by taking aliquots of the reaction mixture and analyzing them at different reaction times. Unfortunately, these analyses revealed an intense peak corresponding to the protonated ligand L1 with *m*/z = 390.2, which dominated the MS even after prolonged reaction times (up to 10 days). The peak corresponding to the protonated complex (*m*/z = 540.1) was only observed as a minor peak, which indicated that complex formation was not efficient. We do not have a definitive explanation for the lack of reactivity of the ligand, but it could be related to very slow complexation kinetics (as observed for DOTA-like ligands in some cases), or perhaps because of a hydrogen-bonding interaction involving the protonated amine of the side chain and the negatively charged carboxylate groups. This interaction occurring on the side of the macrocycle through which the Ln^{3+} ion should enter the cavity of the macrocycle might block the entrance of the metal ion, resulting in very slow complexation kinetics.

SYNTHESIS OF LIGAND L2

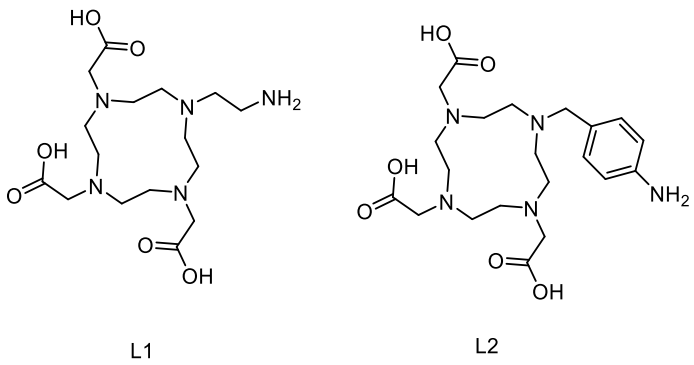

Figure 26. *Comparison of the structures of ligands **L1** and **L2**.*

The synthetic protocol followed for ligand L2 was similar to that used for the synthesis of L1[32]. The starting compound was also DO3AtBu, which was alkylated in the secondary amine of cyclen with 4-nitrobenzenylbromide through a nucleophilic substitution, with a reaction yield of 73%. This intermediate presents the characteristic intense stretching ν(C=O) vibration of the carbonyl groups at 1712 cm^{-1}. The presence of an absorption at 1345 cm^{-1} due to the symmetric stretching vibration of the nitro group (1265-1390 cm^{-1}), and a second band at 1521 cm^{-1} due to the asymmetric stretching of the same group (1495-1580 cm^{-1})[33], confirm the successful alkylation of the DO3A unit. The next step was the reduction of the nitro group with H_2 under Pd/C catalysis to obtain the corresponding amine.[33] Both compounds (nitro and amino derivative) where characterized by ESI-MS along with ^{1}H- and ^{13}C-NMR. The ESI-MS of the final product shows an intense peak (100% BPI) at *m*/*z* = 620.4 due to the (protonated) desired product, together with a second peak (~30% BPI) at *m*/*z* = 642.4

due to the $[NaL2]^+$ entity. This result confirms that both the alkylation of DO3AtBu and the reduction of the nitro group were successful. The ^{1}H-NMR spectrum presents two doublets at 7.12 and 6.57 ppm (^3J = 8.4 Hz) attributed to the aromatic protons of the aminobenzyl group. The spectrum also shows intense signals at 1.41 and 1.39 ppm due to the tertbutyl groups. The signals due to the aliphatic CH_2 protons are observed as relatively broad and poorly defined signals in the range 2.0-4.0 ppm. This is a rather typical behavior observed for cyclen-based ligands, which is related to the conformational rigidity of the macrocyclic scaffold. We also notice that the ^{1}H-NMR spectrum presents two additional doublets in the aromatic region that indicate the presence of a second species with an abundance of ~14%. However, these signals likely correspond to a protonated form of the ligand, as suggested by the presence of a broad signal at 9.84 ppm attributable to a proton inside the macrocyclic cage.

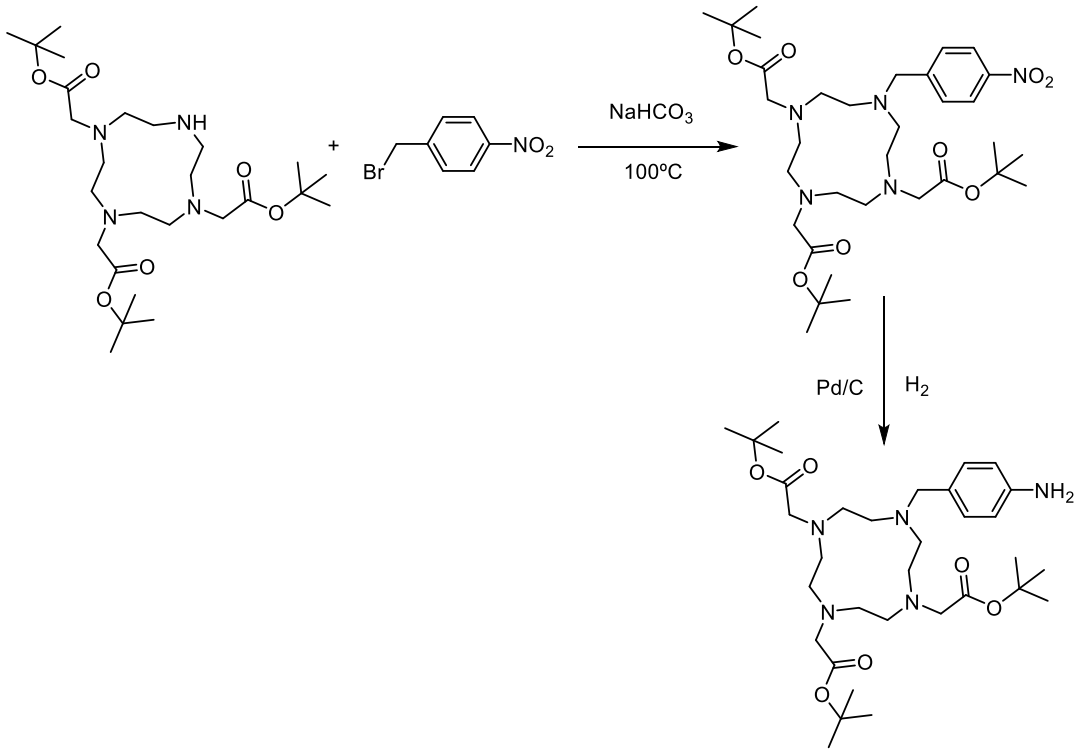

Scheme 5. *Synthetic route for the ligand L2.*

COUPLING OF THE LIGAND L2 TO THE PEPTIDES P1 AND P2

The coupling of L2 to the deprotected carboxylic acid side chain of the Glu residue of both peptides P1 and P2 was carried out in the same way as in the case of L1, except for the fact that in this case the ligand was coupled without previous hydrolysis of the *tert*-butyl groups. This strategy allows minimizing potential side reaction affecting the carboxylate groups of the DO3A unit. The *tert*-butyl groups can be easily removed with the TFA treatment used to cleave the peptide from the resin. The method used for the coupling of the ligand was the activation of the carboxylic group by the *in situ* formation of the activated ester with HBTU, which reacts with the amine group present in L2.

After performing the coupling, a small portion of each resin was analyzed by HPLC (Figure 27). Unfortunately, in these cases it has not been possible to analyze the samples by mass spectrometry, although analyzing the retention times the identity of the products can be qualitatively assigned.

For P1 the HPLC chromatogram shows four peaks in which the peak at t_r = 10.9 min (A), as it has been observed for L1, can be assigned to L2 attached to the peptide, the peak at t_r = 11.4 min (B) can be identified as the unmodified peptide, and the peak at t_r = 12.3 min can correspond to the unmodified peptide in which the free carboxylic acid experienced an intramolecular condensation to form an unreactive lactam (C). Finally, there is a fourth peak at t_r = 13.8 min that may be related with uncomplete *t*-Bu removal by TFA treatment during the cleavage of the peptide from the solid support. The HPLC chromatogram obtained indicates that the desired peptide coupled to L2 was obtained as secondary product.

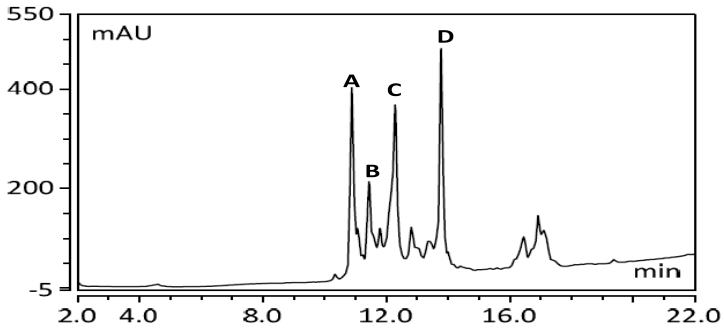

Peak	t_R (min)	Assignment
A	10.9	Product
B	11.4	P1
C	12.3	P1 (-H_2O)
D	13.8	Unhydrolized product

Figure 27. *HPLC chromatogram of the coupling between P1 and L2..*

For the coupling with P2, the HPLC chromatogram shows four major peaks, in which the peak with at t_R = 11.6 min (A) matches with the expected value for the desired product, the one at t_R = 12.3 min surely corresponds with P2 without L2 ligand (B), and the peaks at t_R = 13.4 min and t_R = 14.5 min may be related with the uncomplete *t*-Bu removal. Thus, while incomplete, the analysis of the HPLC chromatograms confirms the coupling of L2 to the envisaged peptides.

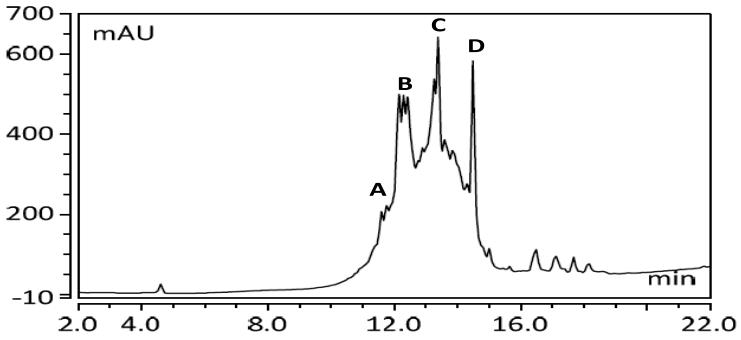

Peak	t_R	Assignment
A	11.6	Product
B	12.3	P2
C	13.4	Unhydrolized product
D	14.5	

Figure 28. *HPLC chromatogram of the coupling between P2 and L2.*

Experimental Part

TIMELINE OF THE WORK

	February				March				April				May				June				July			
	week				*week*				*week*				*week*				*week*				*week*			
	1	2	3	4	1	2	3	4	1	2	3	4	1	2	3	4	1	2	3	4	1	2	3	4
Literature search																								
Peptide synthesis																								
L1 synthesis																								
L1 coupling																								
L2 Synthesis																								
L2 coupling																								
Report redaction																								

General Information

Characterization Techniques

Mass spectra for the characterization of the ligands and for the peptide-ligand couplings were obtained using electrospray ionization technique (positive mode) using *a LC-Q-q-TOF Applied Biosystems QSTAR Elite* mass spectrometer from the Research Support Services (SAI) from the Universidade da Coruña.

For the performed ^{1}H and ^{13}C NMR analyses, a Nuclear Bruker AVANCE III HD 400 belonging to the Research Support Services (SAI-UDC) was used, using $CDCl_3$ and D_2O as solvents for sample preparation.

In order to obtain the IR spectrum, it was registered in a FT.IR spectrophotometer Nicolet iS-10 by Thermo Scientific, equipped with Thermo Scientific Smart iTR using the ATR (Attenuated Total Reflectance) technique, in the Advanced Scientific Research Center (CICA) from Universidade da Coruña.

Reversed-phase HPLC-MS analyses were performed using a *Thermo Scientific UltiMate 3000 instrument,* which was connected to a single quadrupole mass spectrometer *Thermo Scientific MSQ Plus*, and to a PDA (Photo-Diode Array) detector. The solvents used were HPLC-MS quality solvents, A: 0.1% TFA, H_2O and B: 0.1% TFA, ACN. The column used for these analyses was Phenomenex Aeris 3.6 µm peptide XB-C18 100 Å; 150 × 2.1 mm.

The gradient used for reversed-phase HPLC-MS experiments was set as following:

Table 3. *Gradient used for HPLC-MS experiments*

Time (min)	Flow (mL/min)	% B
0	0.300	5
2	0.300	5
25	0.300	95
26	0.300	100
32	0.300	100
33	0.300	5
40	0.300	5

Reagents and Solvents

The solvents used were synthesis grade, obtained from commercial resources, and were used with no additional purification steps. Water was purified using a Milli-Q system (*Millipore*).

Reagent	Trading house
DO3A*t*Bu, pure	CheMatech
N-Boc-bromoethylamine, pure	Carbosynth
K_2CO_3, 99%*	Sigma-Aldrich
$NaHCO_3$, 99%*	Sigma-Aldrich
Pd on activated charcoal 10%	Sigma-Aldrich
Fmoc standard amino acids	Iris Biotech GmbH
Triisopropylsilane, 98%	Acros Organics
N-methylmorpholine, 99%	Acros Organics
4-Methylpiperidine, 99%	Acros Organics
HATU	Iris Biotech GmbH
HBTU	Iris Biotech GmbH
HOBt	Iris Biotech GmbH
Triphenylphosphine, 99%	Sigma-Aldrich
Palladium (II) acetate, 99.98%	Sigma-Aldrich
DIEA, 99%	Sigma-Aldrich
TFA, peptide-synthesis grade	Fisher Bioreagents

*Previously dried in oven

Solvent	Trading House
Acetonitrile, laboratory reagent grade	Fisher Chemical
MeOH, laboratory reagent grade	Fisher Chemical
Dichloromethane, laboratory reagent grade	Fisher Chemical
N,N-Dimethylformamide, peptide-syntheis grade	Sigma-Aldrich

SYNTHESIS

PEPTIDE SYNTHESIS

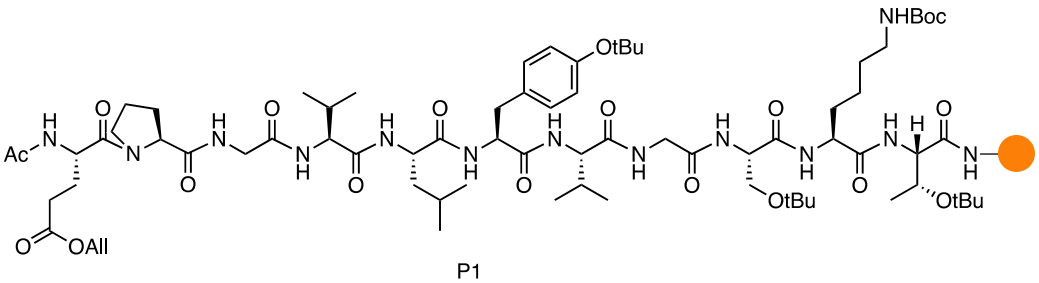

P1

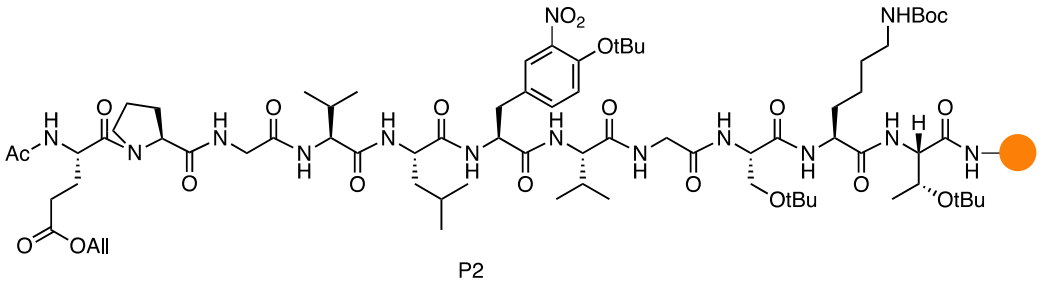

P2

- Resin: H-Rink amide ChemMatrix® resin (0.47 mmol/g)
- Coupling reagent: HBTU/HOBt 0.2 M
- Base: DIEA 0.195 M
- TNBS protection/deprotection test for the amine group: 1 % TNBS/DMF + 10% DIEA/DMF
- Fmoc removal agent: 4-methylpiperidine
- Sequence: Glu-Pro-Gly-Val-Leu-Tyr-Val-Gly-Ser-Lys-Thr (Ac-EPGVLYVGSKT-NH_2).

First, the resin (0.1 mmol, 212.7 mg) was placed in a plastic column for SPPS and washed twice, one with DCM and the other one with DMF under N_2 bubbling (Figure 29A). Then, a TNBS test was done in order to check that the amine group was deprotected (positive result). The protected amino acid Fmoc-Thr(*t*Bu)-OH (in excess, 4 eq) was dissolved in 0.2 M HBTU/HOBt in DMF (4 eq, 2 mL) and then a 0.195 M DIEA solution in DMF (6 eq, 3 mL) was added. After 2 min mixing for the activation of the carboxylic acid, the solution was added to the resin and mixed under N_2 bubbling for 30 min. Afterwards, the solvent was removed by filtration (figure 29B), the resin was washed with DMF (2 × 5 mL), and then a TNBS test was performed to check the efficiency of the coupling, showing in this case a negative result. Finally, the Fmoc protecting group was removed by treatment with 20 % 4-methylpiperidine in DMF (in excess, 5 mL) during 15 min. The resin was again filtered and washed three times, two with DCM and one with DMF, and then a TNBS test showed again positive result. This procedure was repeated for each amino acid of the peptide sequence, forming the peptide from the *C*-terminus to the *N*-terminus.

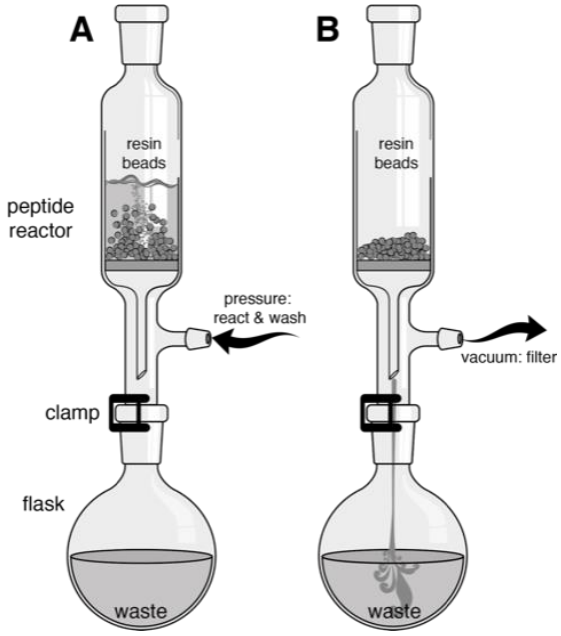

***Figure 29**. Assembly used for SPPS.*

ALLYL GROUP DEPROTECTION

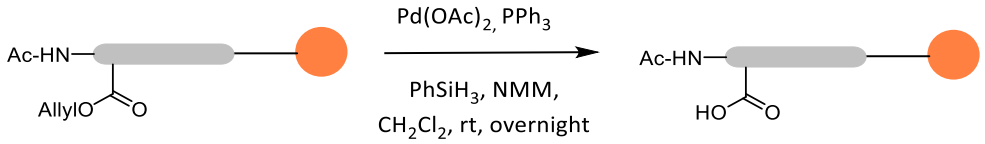

The resin with the synthesized peptide (0.05 mmol, 61,5 mg) was treated with a mixture of $Pd(OAc)_2$ (0.015 mmol, 3.4 mg), PPh_3 (0.075 mmol, 19.7 mg), $PhSiH_3$ (0.5 mmol, 62 µL) and NMM (0.5 mmol, 55 µL) in DCM (2.5 mL), the solution was mixed overnight under mechanic stirring. Afterwards, the resin was filtered and washed as follow: DCM (2 × 2 mL × 2 min), DMF (2 × 2 mL × 2 min), DEDTC (25 mg/5 mL DMF × 15 min), DMF (2 × 2 mL × 2 min), and DCM (2 × 2 mL × 2 min).

L1

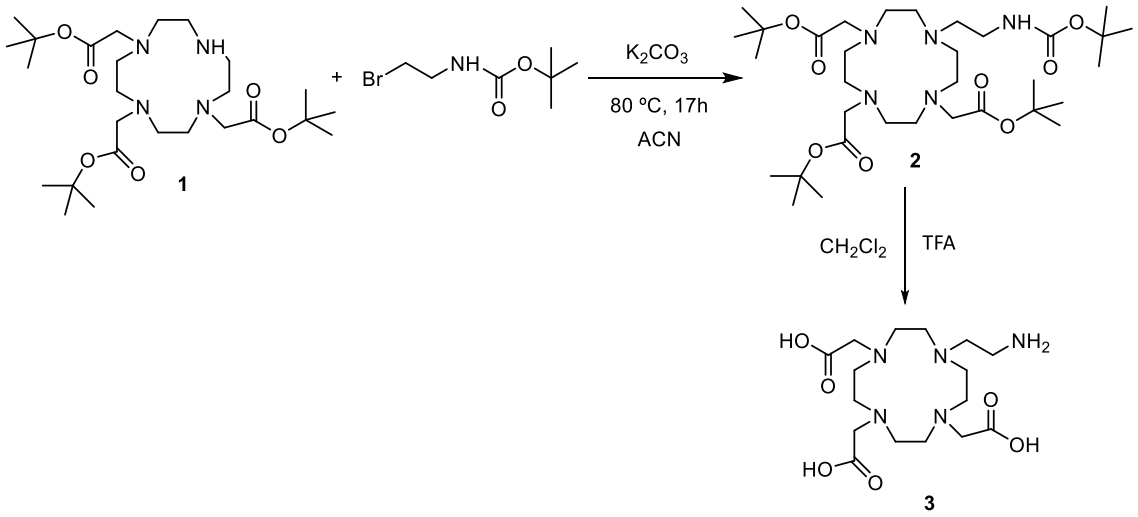

In order to obtain L1, compound **1** (DO3A*t*Bu) (0.97 mmol, 500 mg) and *N*-Boc-2-bromoethylamine (0.97 mmol, 224 mg) were dissolved in 25 mL of ACN. Then, K_2CO_3 (2.5 mmol, 335 mg) was added to the mixture and the solution was stirred under reflux for 17 h. Then, the solution was filtrated and the filtrate was concentrated to dryness under reduced pressure. A yellowish oil, identified as compound **2**, was obtained (460 mg, 72%).

ESI-MS: m/z (I%) 658.5 (100%) $[MH]^+$.

Compound **2** was dissolved in 10 mL of TFA:CH_2Cl_2 (1:1) and the resulting mixture was stirred overnight**.** The solution was then concentrated under reduced pressure and washed with water several times. Compound **3** (**L1**) was obtained as a clear yellow solid after purification with reversed-phase MPLC (265.7 mg, 97.7%). The overall process yield was 70%.

ESI-MS: *m/z* (I%) 390.3 (100%) $[MH]^+$, 428.18 (41%) $[MK]^+$.

^{13}C-NMR: (ppm) 174.37, 170.07, 66.08, 56.17, 53.03, 51.94, 50.46, 50.01, 49.14, 48.33, 47.65, 42.22, 40.65, 36.19, 34.49 .

P1-L1 COUPLING

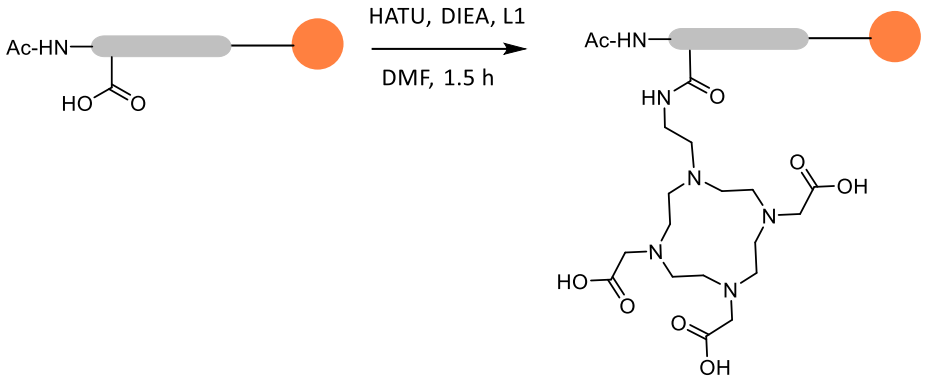

P1 resin (0.0084 mmol, 30 mg) was placed in an Eppendorf tube and 240 µL of DMF were added along with 0.195 M DIEA in DMF (0.0126 mmol, 64 µl) and HATU (0.0084 mmol, 3.2 mg). The resulting mixture was mixed for 3 min for its activation, and then L1 (0.042 mmol, 16.35 mg) was added and the mixture stirred for 1.5 h. Finally, the resin was filtered and washed with DCM (2 × 1 mL × 2 min).

For the HPLC analysis, 3-4 mg of the resin were treated with 150 µL of the cleaving cocktail (2.5% triisopropylsilane, TIS, 2.5% H_2O, and 95% TFA) for 1.5 h. Then, the resin was filtered, the filtrate was placed in ice-cold ether (1.2 mL), and then the solution was centrifuged for 5 min. The precipitate was dissolved in 400 µL of H_2O:MeCN (1:1) and analysed by reversed-phase HPLC-MS.

t_R = 10.9 min (column *Phenomenex Aeris peptide XB-C18*, lineal gradient 5→95 % ACN, 0.1 % TFA / H2O, 0.1 % TFA in 23 min).

ESI-MS (m/z) for $C_{70}H_{116}N_{18}O_{22}$ calculated 1561.8 $[MH]^+$; found 781.4 $[MH_2]^{2+}$

P2-L1 COUPLING:

P2 resin (0.0084 mmol, 30 mg) was placed in an Eppendorf tube, 240 µl of DMF were added along with 0.195 M DIEA in DMF (0.0126 mmol, 64 µl) and HATU (0.0084 mmol, 3.2 mg). The resulting mixture was mixed for 3 min for its activation, and then L1 (0.042 mmol, 16.35 mg) was added and the mixture stirred for 1.5 h. Finally, the resin was filtered and washed with DCM (2 × 1 mL × 2 min).

For its HPLC analysis, 3-4 mg of the resin were treated with 150 µL of the cleaving cocktail (2.5% triisopropylsilane, TIS, 2.5% H_2O, and 95% TFA) for 1.5 h. Then, the resin was filtered, the filtrate was placed in ice-cold ether (1.2 mL), and then the solution was centrifuged for 5 min. The precipitate was dissolved in 400 µL of H_2O:MeCN (1:1) and analysed by reversed-phase HPLC-MS.

t_R = 11.6 min (column *Phenomenex Aeris peptide XB-C18*, lineal gradient 5→95 % ACN, 0.1 % TFA / H2O, 0.1 % TFA in 23 min).

ESI-MS (m/z) for $C_{70}H_{115}N_{19}O_{24}$ calculated 1606.8 $[MH]^+$; found 804.5 $[MH_2]^{2+}$

L2

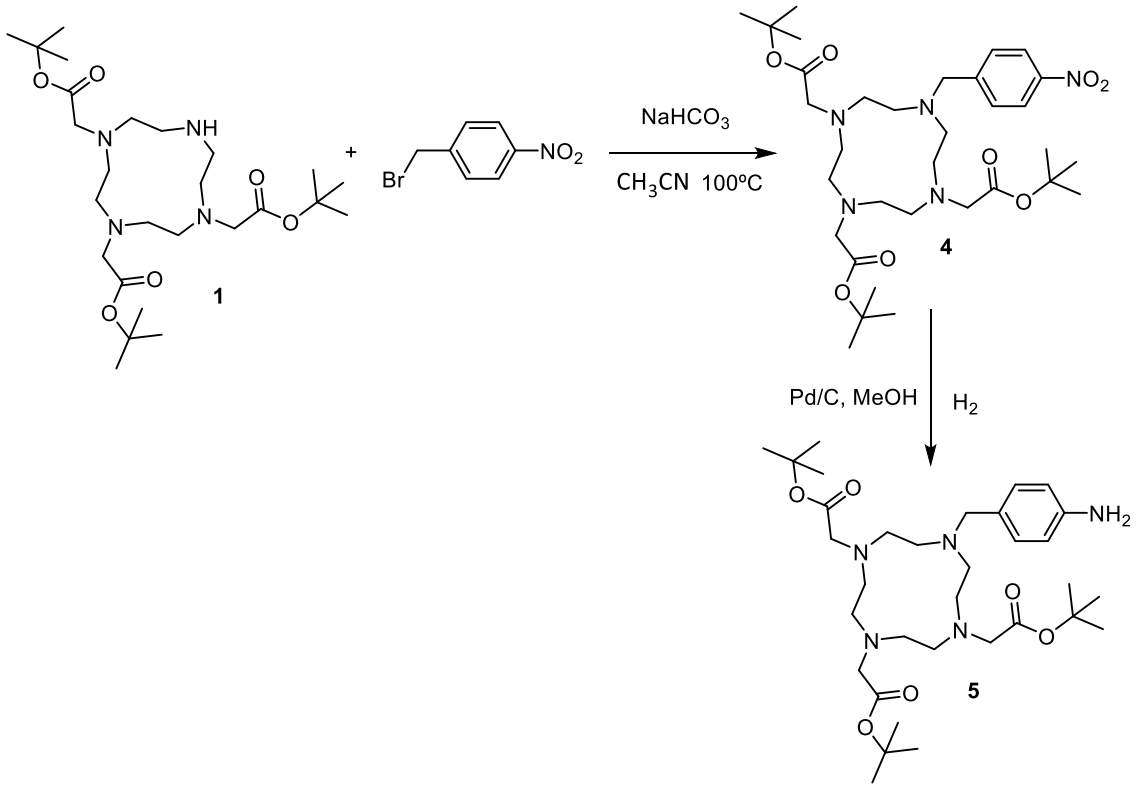

Compound **1** (0.97 mmol, 500 mg) and 4-nitrobenzylbromide (0.97 mmol, 210 mg) were dissolved in ACN (25 mL) and $NaHCO_3$ (3.9 mmol, 326 mg) was added to the mixture. The solution was stirred for 14 h under reflux. Then, the solvent was removed under reduced pressure and the crude was purified by column chromatography using SiO_2 with $MeOH/CH_2Cl_2$ (5:95) as the mobile phase.

ESI-MS: *m/z* (I%) 650.4 (49%) $[MH]^+$, 672.4 (100%) $[MNa]^+$

IR: (cm^{-1}) $\nu_{as}(NO_2)$ = 1512 , $\nu_s(NO_2)$ = 1345 ν(C=O) = 1712 ν(C-H) = 2932

Compound **4** (0.31 mmol, 200 mg) was reduced under H_2 atmosphere with Pd/C catalysis in 10 mL of methanol for 12 h. Then, the solvent was removed under reduced pressure obtaining Compound **5** (**L2**).

ESI-MS: *m/z* (I%) 620.4 (70%) $[MH]^+$.

^{1}H-NMR (400 MHz, $CDCl_3$) δ (ppm): 1.40 (m, 38H), 2.98 (m, 36H), 6.57 (d, 2H, J = 8.9 Hz), 6.87 (m, 1H), 7.12 (d, 2H, J = 8.7 Hz).

^{13}C-NMR: (ppm) 173.29, 172.34, 170.55, 169.65, 146.22, 143.97, 130.88, 129.60, 127.36, 126.29, 115.18, 115.04, 112.50, 82.74, 82.29, 81.66, 81.46, 77.45, 58.86, 57.97, 55.83,

55.62, 53.53, 51.16, 49.03, 47.41, 31.83, 29.59, 28.16, 28.13, 27.93, 27.82, 22.60, 20.38, 14.05.

P1-L2 COUPLING

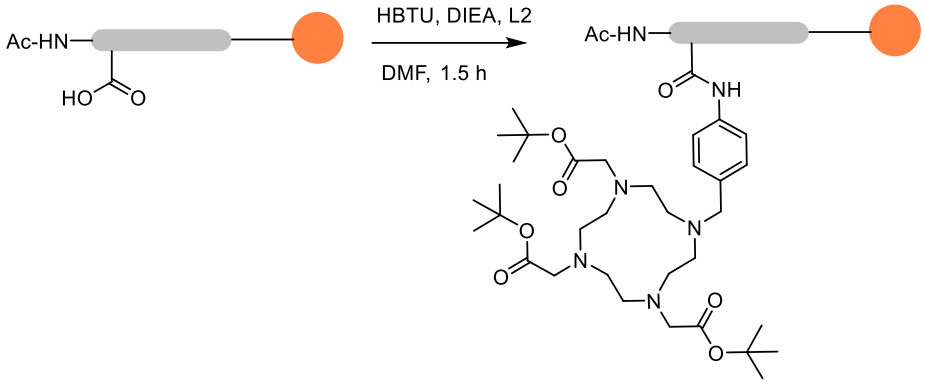

P1 resin (0.0084 mmol, 30 mg) was placed in an Eppendorf tube, 250 µl of DMF were added along with 0.195 M DIEA in DMF (0.0168 mmol, 86 µl) and HBTU (0.0084 mmol, 3.2 mg). The resulting mixture was mixed for 3 min for its activation, and then L2 (0.042 mmol, 26 mg) was added and the mixture stirred for 1.5 h. Finally, the resin was filtered and washed with DCM (2 × 1 mL × 2 min).

For its HPLC analysis, 3-4 mg of the resin were treated with 150 µL of the cleaving cocktail (2.5% triisopropylsilane, TIS, 2.5% H_2O, and 95% TFA) for 4 h. Then, the resin was filtered, the filtrate was placed in ice-cold ether (1.2 mL), and then the solution was centrifuged for 5 min. The precipitate was dissolved in 400 µL of H_2O/MeCN (1:1) and analysed by reversed-phase HPLC-MS.

t_R = 10.9 min (column *Phenomenex Aeris peptide XB-C18*, lineal gradient 5→95 % ACN, 0.1 % TFA / H2O, 0.1 % TFA in 23 min).

P2-L2 COUPLING

P2 resin (0.0084 mmol, 30 mg) was placed in an Eppendorf tube, 250 µl of DMF were added along with 0.195 M DIEA in DMF (0.0168 mmol, 86 µl) and HBTU (0.0084 mmol, 3.2 mg). The resulting mixture was mixed for 3 min for its activation, and then L2 (0.042 mmol, 16.35 mg) was added and the mixture stirred for 1.5 h. Finally, the resin was filtered and washed with DCM (2 × 1 mL × 2 min).

For its HPLC analysis, 3-4 mg of the resin were treated with 150 µL of the cleaving cocktail (2.5% triisopropylsilane, TIS, 2.5% H_2O, and 95% TFA) for 4 h. Then, the resin was filtered, the filtrate was placed in ice-cold ether (1.2 mL), and then the solution was centrifuged for 5 min. The precipitate was dissolved in 400 µL of H_2O:MeCN (1:1) and analysed by reversed-phase HPLC-MS.

t_R = 11.6 min (column *Phenomenex Aeris peptide XB-C18*, lineal gradient 5→95 % ACN, 0.1 % TFA / H2O, 0.1 % TFA in 23 min).

Conclusions

This work has focused on the design and synthesis of potential luminescent sensors for oxidative stress, based on small peptide units coupled to DO3A units for the coordination to a luminescent Eu^{3+} ion. Our design relies on the lower pK_a of the phenol group of a tyrosine group upon nitration. Deprotonation of the nitrated peptide is expected to cause coordination of the nitrophenyl group to the lanthanide ion, allowing the luminescent sensitization of the lanthanide through the antenna effect. The work presented in this report focused on the synthesis of the two main components of the sensor, peptides P1 and P2, and a DO3A unit functionalized with an amine group. The analysis of the experimental results provides the following conclusions:

- Two DOTA ligand derivatives containing amine were successfully synthesized, 2,2',2''-(10-(2-aminoethyl)-1,4,7,10-tetraazacyclododecane-1,4,7-triyl)triacetic acid (**L1**) and tri-tert-butyl 2,2',2''-(10-(4-aminobenzyl)-1,4,7,10-tetraazacyclododecane-1,4,7-triyl)triacetate (**L2**).
- Ligand L1 was found to be particularly inefficient in the formation of complexes with the Eu^{3+} ion, suggesting that the presence of the ethylamine arm interferes in the complexation process, which was found to be extremely slow.
- Two peptides derived from α-synuclein (EPGVL**Y**VGSKT and EPGVL**nY**VGSKT), were synthesized by SPPS. One of them contains a nitrated tyrosine residue (nY) in order to study the use of this chromophore as lanthanide sensitizer.

HPLC-MS analysis confirmed that both ligands were coupled to both peptides in the carboxylic acid group of the side chain of the Glu residue. However, the coupling reaction conditions must be optimized in order to improve the yield of the desired products and reduce the formation of the unreactive lacta

Conclusiones

Este Trabajo de Fin de Grado se centró en el diseño y síntesis de un potencial sensor luminiscente para el estrés oxidativo, basado en pequeños péptidos acoplados a unidades DO3A para la coordinación del ion Eu^{3+}. El diseño se sustenta en el menor pK_a del grupo fenol de un grupo tirosina una vez que sufre un proceso de nitración. La desprotonación del péptido nitrado es de esperar que provoque la coordinación del grupo cromóforo nitrofenilo al ion lantánido, permitiendo su excitación mediante el conocido efecto antena. El trabajo presentado en esta memoria se centró en la síntesis de los dos componentes principales del sensor, los péptidos P1 e P2, y la unidad DO3A funcionalizada con un grupo amino para su acoplamiento con los péptidos. El análisis de los resultados experimentales permitió llegar a las siguientes conclusiones:

- Dos ligandos derivados del compuesto DOTA, fueron sintetizados con éxito, el ácido 2,2',2''-(10-(2-aminoetil)-1,4,7,10-tetraazacyclododecano-1,4,7-triil)triacetico (L1) y el tri-tert-butil 2,2',2''-(10-(4-aminobencil)-1,4,7,10-tetraazacyclododecano-1,4,7-triil)triacetato (L2).
- El ligando L1 es particularmente ineficiente en la complejación del ion Eu^{3+}, lo que sugiere que la presencia del brazo etilamina interfiere de alguna manera en el proceso de complejación, que es extraordinariamente lento.
- Dos péptidos, EPGVL**Y**VGSKT y EPGVL**nY**VGSKT derivados de α-sinucleína, se sintetizaron por SPPS. Uno de ellos contiene un residuo de tirosina nitrado (nY) para estudiar el uso de este cromóforo como sensibilizador de lantánidos.
- Se confirmó por HPLC-MS que ambos ligandos se acoplaron a ambos péptidos en el ácido carboxílico de la cadena lateral del residuo de Glu. Sin embargo, las condiciones de la reacción de acoplamiento deben optimizarse para mejorar el rendimiento de los productos deseados y reducir la formación de las lactamas no reactivas.

. Conclusións

Este Traballo de Fin de Grao centrouse no deseño e síntese dun potencial sensor luminescente para o estres oxidativo, baseado en pequenos péptidos acoplados a unidades DO3A para a coordinación do ion Eu^{3+}. O deseño susténtase no menor pK_a do grupo fenol dun grupo tirosina unha vez que sofre un proceso de nitración. A deprotonación do péptido nitrado é de esperar que provoque a coordinación do grupo cromofórico nitrofenilo ao ion lantánido, permitindo a súa excitación mediante o coñecido efecto antena. O traballo presentado nesta memoria centrouse na síntese dos dous compoñentes principais do sensor, os péptidos P1 e P2, e a unidade DO3A funcionalizada cun grupo amino para o seu acoplamento cos péptidos. A análise dos resultados experimentais permitiu chegar ás seguintes conclusións:

- Dous ligandos derivados do DOTA, foron sintetizados con éxito, o ácido 2,2',2''-(10-(2-aminoetil)-1,4,7,10-tetraazacyclododecano-1,4,7-triil)triacetico (L1) e o tri-tert-butil 2,2',2''-(10-(4-aminobencil)-1,4,7,10-tetraazacyclododecano-1,4,7-triil)triacetato (L2).
- O ligando L1 é particularmente ineficiente na complexación do ion Eu^{3+}, o que suxire que a presenza do brazo etilamina interfire dalgunha maneira no proceso de complexación, que é extraordinariamente lento.
- Dous péptidos, EPGVL**Y**VGSKT e EPGVL**nY**VGSKT derivados de α-sinucleina, foron sintetizados mediante SPPS. Un deles contén un residuo de tirosina nitratado (nY) para estudar o uso deste cromóforo como un sensibilizador de lantánidos.
- Confirmouse por HPLC-MS que ambos ligandos foron acoplados a ambos péptidos no ácido carboxílico da cadea lateral do residuo de Glu. Non obstante, as condicións da reacción do acoplamento deben optimizarse para mellorar o rendemento dos produtos desexados e reducir a formación das lactamas non reactivas.

References

(1) Poewe, W.; Seppi, K.; Tanner, C. M.; Halliday, G. M.; Brundin, P.; Volkmann, J.; Schrag, A. E.; Lang, A. E. Parkinson Disease. *Nature* **2017**, 3.

(2) Nieoullon, A. Neurodegenerative Diseases and Neuroprotection: Current Views and Prospects. *J. Appl. Biomed.* **2011**, *9* (4), 173–183.

(3) Goedert, M. Alzheimer's and Parkinson's Diseases: The Prion Concept in Relation to Assembled Aβ, Tau, and α-Synuclein. *Science (80-.).* **2015**, *349* (6248).

(4) Betteridge, D. J. What Is Oxidative Stress? *Metabolism.* **2000**, *49* (2 SUPPL. 1), 3–8.

(5) Ferrer-Sueta, G.; Campolo, N.; Trujillo, M.; Bartesaghi, S.; Carballal, S.; Romero, N.; Alvarez, B.; Radi, R. Biochemistry of Peroxynitrite and Protein Tyrosine Nitration. *Chem. Rev.* **2018**, *118* (3), 1338–1408.

(6) Giasson, B. I.; Duda, J. E.; Murray, I. V. J.; Chen, Q.; Souza, J. M.; Hurtig, H. I.; Ischiropoulos, H.; Trojanowski, J. Q.; Lee, V. M. Y. Oxidative Damage Linked to Neurodegeneration by Selective Alpha-Synuclein Nitration in Synucleonopathy Lesions. *Science* **2000**, *290* (November), 985–989.

(7) Vollhardt, P.; Schore, N. *Organic Chemistry Structure and Function*, 7th editio.; 2014.

(8) Chakraborty, P.; Onufriev, A. A Computational Framework for Interacting with Physical Molecular Models of the Polypeptide Chain Molecular Models of the Polypeptide Chain. **2014**.

(9) Devlin, T. M. *Textbook of Biochemistry with Clinical Correlations*, 6th editio.; Delvin, T. D., Ed.; Wiley-Liss, 2006.

(10) Whitford, D. *Proteins. Structure and Function*; John Wiley & Sons Ltd., 2005.

(11) Banci, L.; Cantini, F. 2 Structure of Biomolecules: Fundamentals 2.1. **2012**.

(12) Elliott, W. H.; Elliott, D. C. *Biochemistry and Molecular Biology*; Oxford University Press: New York, 2009.

(13) Hruby, V.; Meyer, J.-P. *Bioorganic Chemistry, Peptides and Proteins*; Sydney M., H., Ed.; Oxford University Press: New York, 1998.

(14) T. Scott, Y.; Barany, G. *Solid-Phase Synthesis, A Practical Guide*; Steven A., K., Albericio, F., Eds.; Marcel Dekker, Inc., 2000.

(15) Isidro-Llobet, A.; Álvarez, M.; Albericio, F. Amino Acid-Protecting Groups. *Chem. Rev.* **2009**, *109* (6), 2455–2504.

(16) El-Faham, A.; Albericio, F. Peptide Coupling Reagents, More than a Letter Soup. *Chem. Rev.* **2011**, *111* (11), 6557–6602.

(17) Platas-Iglesias, C. Caracterización Estructural Y Propiedades Fotofísicas de Complejos de Lantánidos Con Nuevos Receptores Macrocíclicos., University of A Coruña, 1999.

(18) Atkins, P.; Overton, T. *Shiver & Atkin´s Inorganic Chemistry*, 5th ed.; Oxford University: Oxford, 2010.

(19) Shannon, R. D. Revised Effective Ionic Radii and Systematic Studies of Interatomic Distances in Halides and Chalcogenides. *Acta Crystallogr. Sect. A* **1976**, *32* (5), 751–767.

(20) Pearson, R. G. Hard and Soft Acids and Bases. *J. Am. Chem. Soc.* **1963**, *85* (22), 3533–3539.
(21) Regueiro-Figueroa, M.; Nonat, A.; Rolla, G. A.; Esteban-Gõmez, D.; De Blas, A.; Rodríguez-Blas, T.; Charbonnière, L. J.; Botta, M.; Platas-Iglesias, C. Self-Aggregated Dinuclear lanthanide(III) Complexes as Potential Bimodal Probes for Magnetic Resonance and Optical Imaging. *Chem. - A Eur. J.* **2013**, *19* (35), 11696–11706.
(22) Sy, M.; Nonat, A.; Hildebrandt, N.; Charbonnière, L. J. Lanthanide-Based Luminescence Biolabelling. *Chem. Commun.* **2016**, *52* (29), 5080–5095.
(23) Burai, L.; Fabian, I.; Kiraly, R.; Szilagyi, E.; Brucher, E. Equilibrium and Kinetic Studies on the Formation of the lanthanide(III) Complexes, [Ce(dota)]2 and [Yb(dota)]2 (H4dota 5 1,4,7,10-Tetraazacyclododecane-1,4,7,10-Tetraacetic Acid). *J. Chem. Soc., Dalt. Trans.* **1998**, 243–248.
(24) Valeur, B. *Molecular Fluorescence Principles and Applications*; 2001; Vol. 8.
(25) Bünzli, J. C. G. Lanthanide Luminescence for Biomedical Analyses and Imaging. *Chem. Rev.* **2010**, *110* (5), 2729–2755.
(26) Bünzli, J.-C. G.; Piguet, C. Taking Advantage of Luminescent Lanthanide Ions. *Chem. Soc. Rev.* **2005**, *34* (12), 1048.
(27) Caravan, P.; Ellison, J. J.; McMurry, T. J.; Lauffer, R. B. Gadolinium(III) Chelates as MRI Contrast Agents: Structure, Dynamics, and Applications. *Chem. Rev.* **1999**, *99* (9), 2293–2352.
(28) Pazos, E.; Goličnik, M.; Mascareñas, J. L.; Eugenio Vázquez, M. Detection of Phosphorylation States by Intermolecular Sensitization of Lanthanide-Peptide Conjugates. *Chem. Commun.* **2012**, *48* (76), 9534–9536.
(29) Ito, H.; Terai, T.; Hanaoka, K.; Ueno, T.; Komatsu, T.; Nagano, T.; Urano, Y. Detection of NAD(P)H-Dependent Enzyme Activity with Dynamic Luminescence Quenching of Terbium Complexes. *Chem. Commun.* **2015**, *51* (39), 8319–8322.
(30) Chavarría, C.; Souza, J. M. Oxidation and Nitration of α-Synuclein and Their Implications in Neurodegenerative Diseases. *Arch. Biochem. Biophys.* **2013**, *533* (1–2), 25–32.
(31) Carron, S.; Li, Q. Y.; Vander Elst, L.; Muller, R. N.; Parac-Vogt, T. N.; Capobianco, J. A. Assembly of near Infra-Red Emitting Upconverting Nanoparticles and Multiple Gd(iii)-Chelates as a Potential Bimodal Contrast Agent for MRI and Optical Imaging. *Dalt. Trans.* **2015**, *44* (25), 11331–11339.
(32) Mizukami, S.; Tonai, K.; Kaneko, M.; Kikuchi, K. Lanthanide-Based Protease Activity Sensors for Time-Resolved Fluorescence Measurements Lanthanide-Based Protease Activity Sensors for Time-Resolved Fluorescence. *Society* **2008**, 14376–14377.
(33) Zhang, K.; Dou, W.; Tang, X.; Yang, L.; Ju, Z.; Cui, Y.; Liu, W. Selective and Sensitive Time-Gated Luminescence Detection of Hydrogen Sulfide. *Tetrahedron Lett.* **2015**, *56* (21), 2707–2709.

Annex

COMPOUND 2

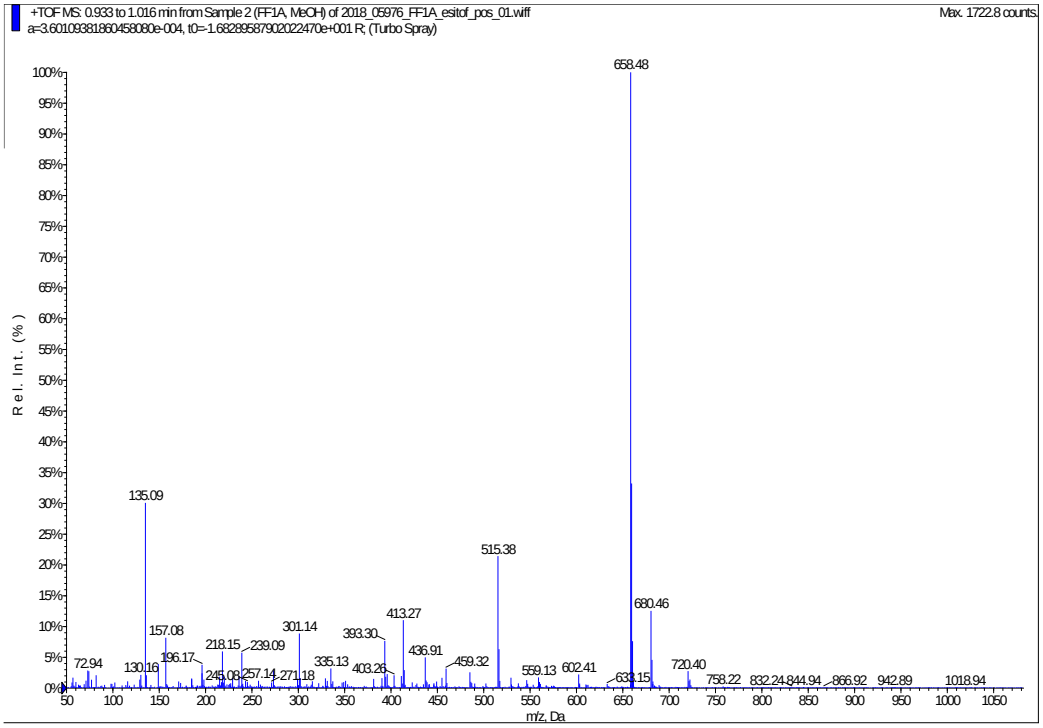

COMPOUND 3, L1

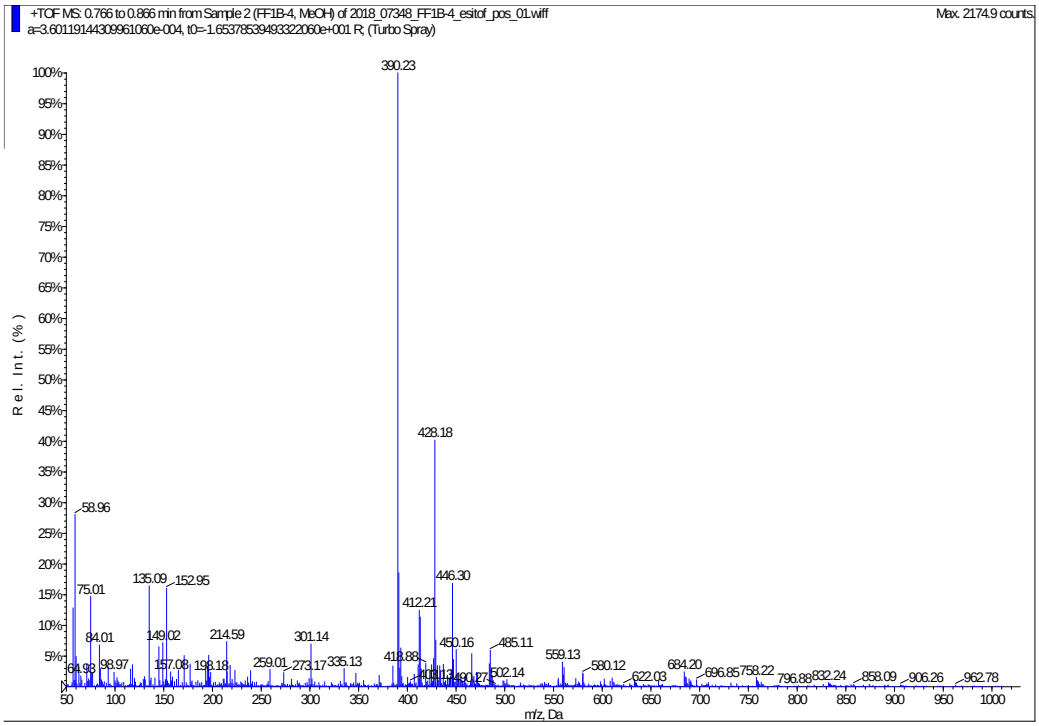

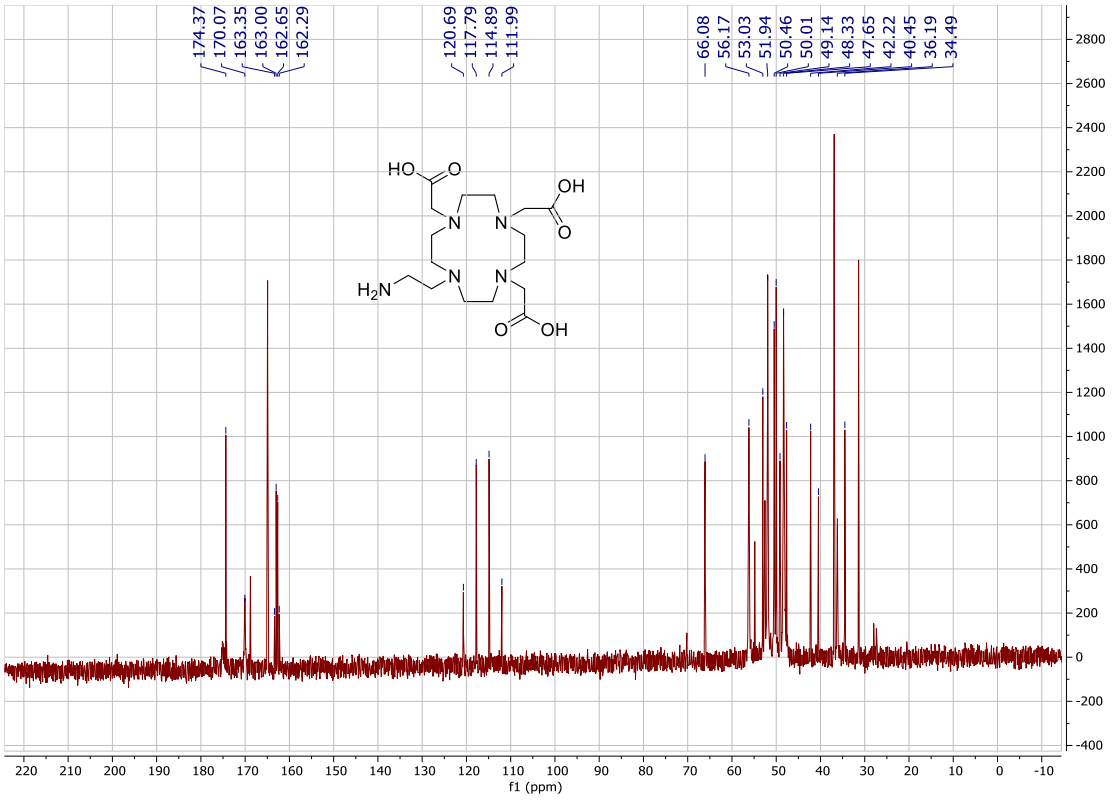
174.37
170.07
163.35
163.00
162.65
162.29
120.69
117.79
114.89
111.99
66.08
56.17
53.03
51.94
50.46
50.01
49.14
48.33
47.65
42.22
40.45
36.19
34.49
HO
O
OH
O
N
N
N
N
H_2N
O
OH
f1 (ppm)

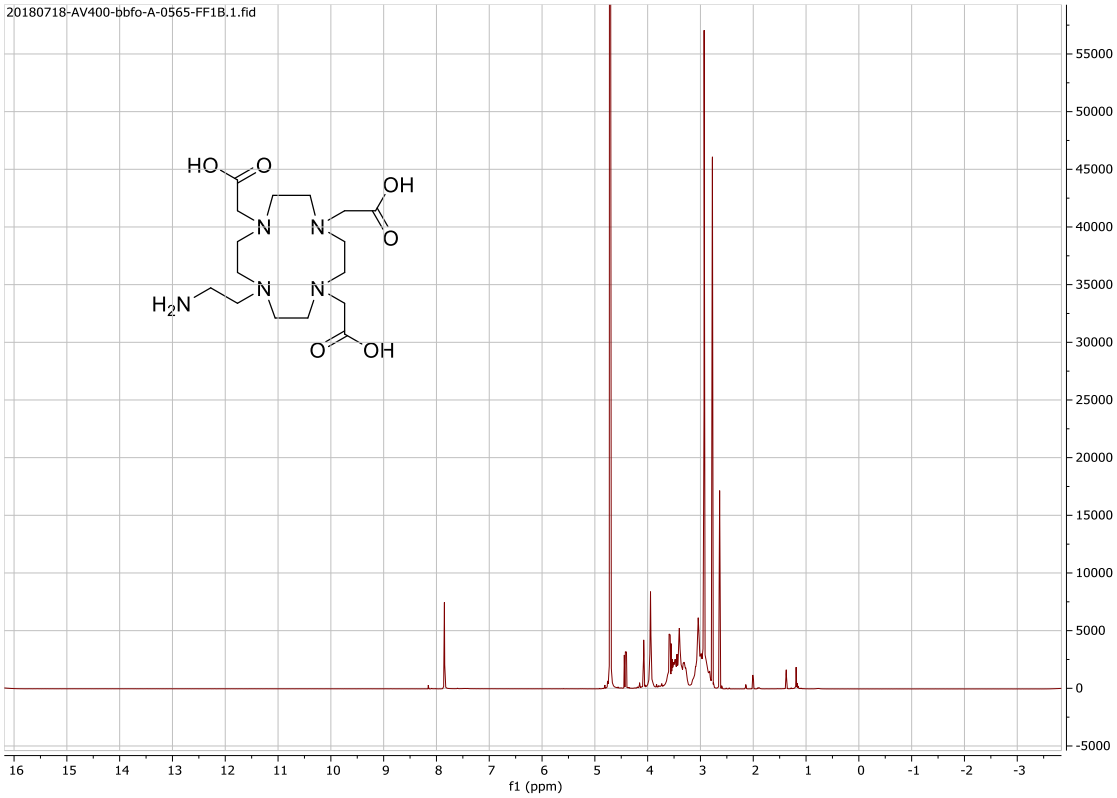
20180718-AV400-bbfo-A-0565-FF1B.1.fid
HO
O
OH
O
N
N
N
N
H_2N
O
OH
f1 (ppm)

P1-L1

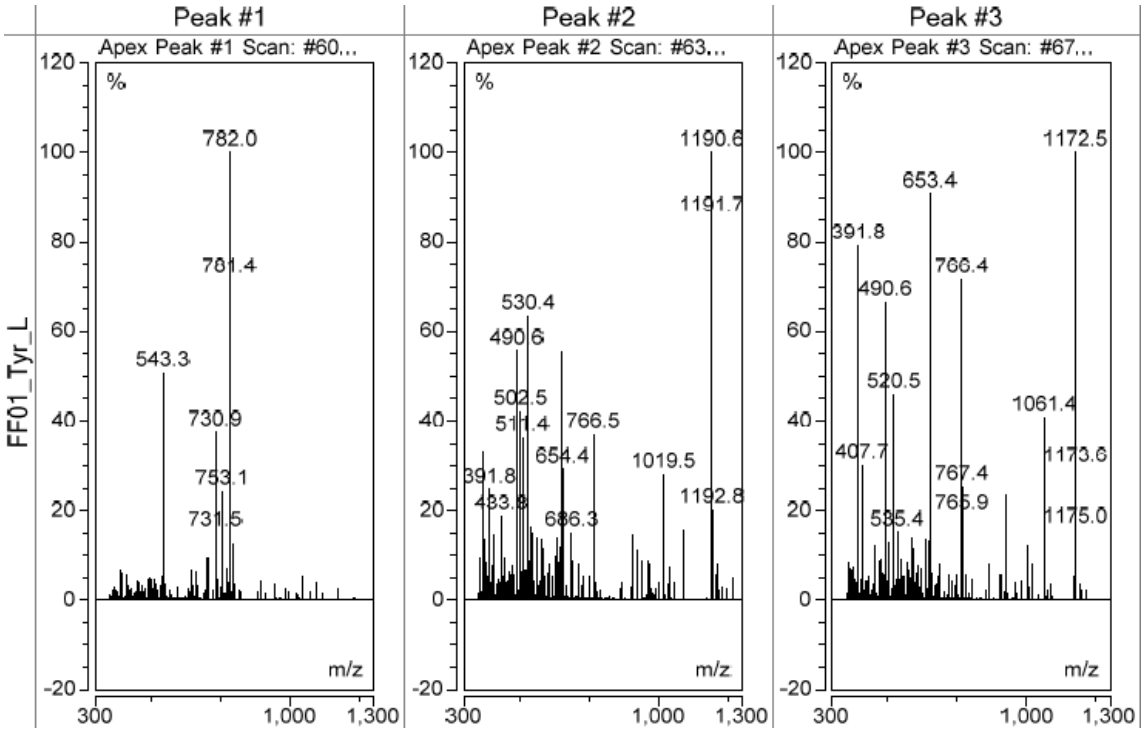
Peak #1
Apex Peak #1 Scan: #60...
Peak #2
Apex Peak #2 Scan: #63...
Peak #3
Apex Peak #3 Scan: #67...
FF01_Tyr_L
%
m/z
782.0
781.4
543.3
730.9
753.1
731.5
1190.6
1191.7
530.4
490.6
502.5
511.4
766.5
654.4
1019.5
391.8
493.8
686.3
1192.8
1172.5
653.4
391.8
766.4
490.6
520.5
1061.4
407.7
1173.6
767.4
765.9
535.4
1175.0

P2-L1

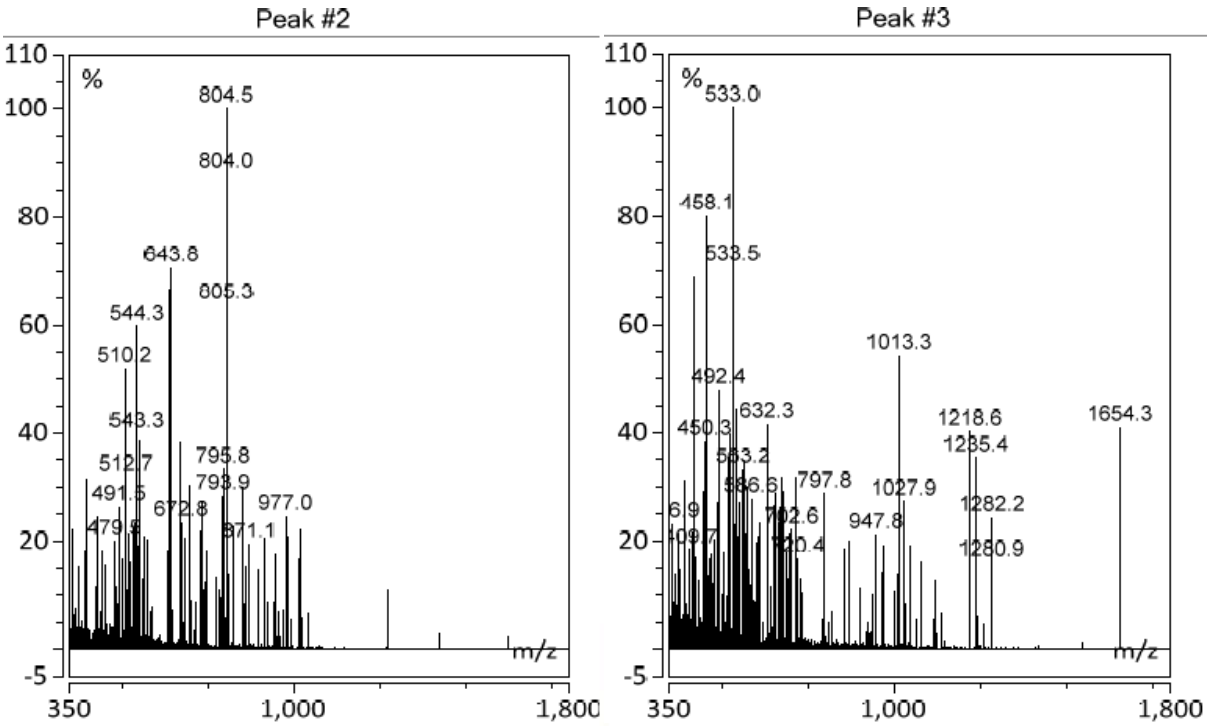
Peak #2
Peak #3
%
m/z
804.5
804.0
643.8
805.3
544.3
510.2
543.3
512.7
795.8
793.9
491.5
672.8
977.0
479.8
671.1
533.0
458.1
533.5
1013.3
492.4
632.3
450.3
1218.6
1654.3
1235.4
563.2
797.8
1027.9
1282.2
947.8
1280.9

COMPOUND 4

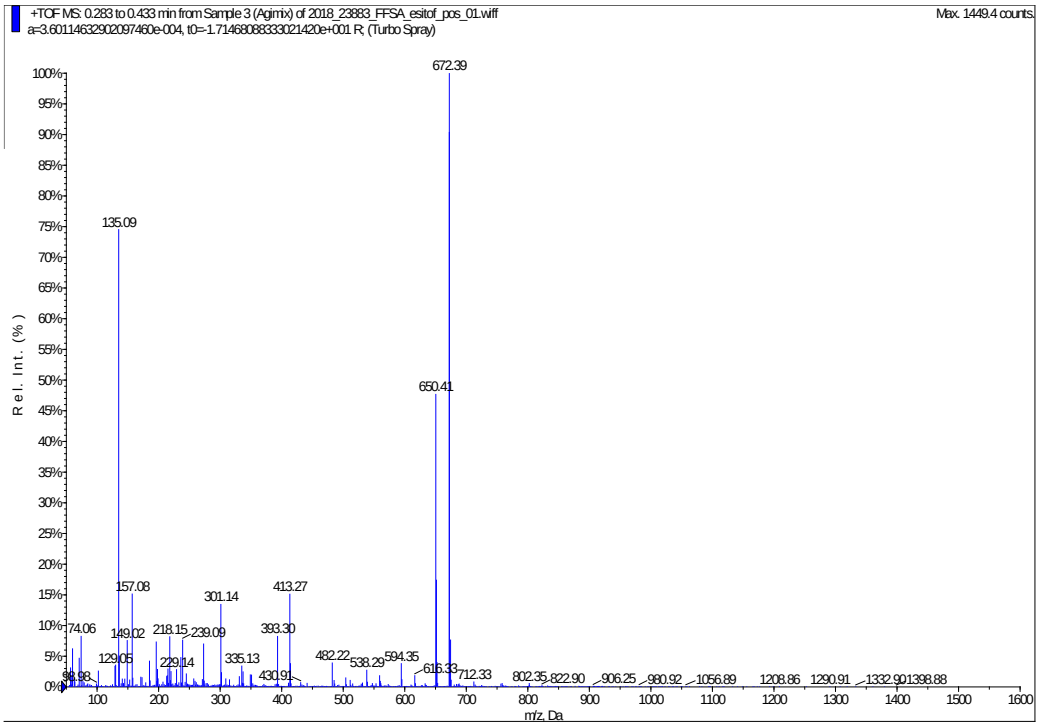
+TOF MS: 0.283 to 0.433 min from Sample 3 (Agimix) of 2018_23883_FFSA_esitof_pos_01.wiff
a=3.601146329020974 60e-004, t0=-1.714680883330214 20e+001 R, (Turbo Spray)
Max. 1449.4 counts.
Rel. Int. (%)
m/z, Da
672.39
650.41
135.09
157.08
301.14
413.27
74.06
149.02
218.15
239.09
393.30
129.05
229.14
335.13
430.91
482.22
538.29
594.35
616.33
712.33
802.35
822.90
906.25
980.92
1056.89
1208.86
1290.91
1332.90
1398.88

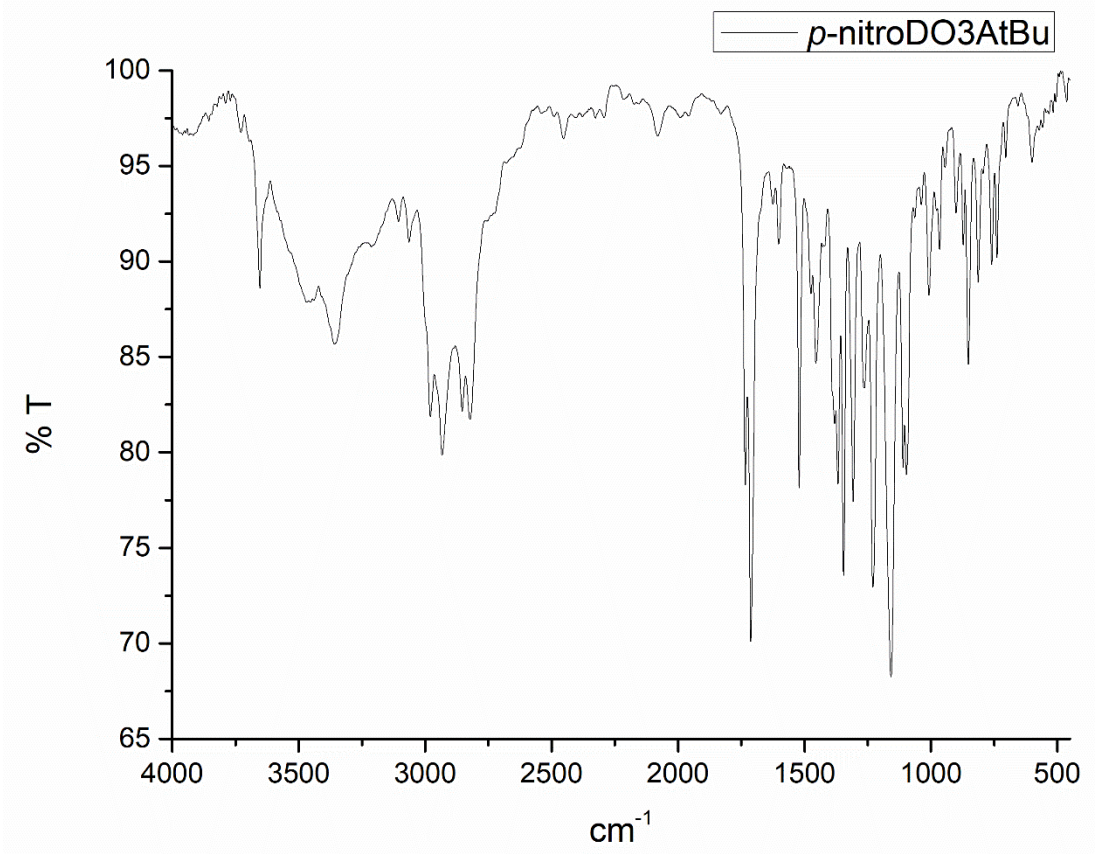
p-nitroDO3AtBu
% T
cm-1

COMPOUND 5

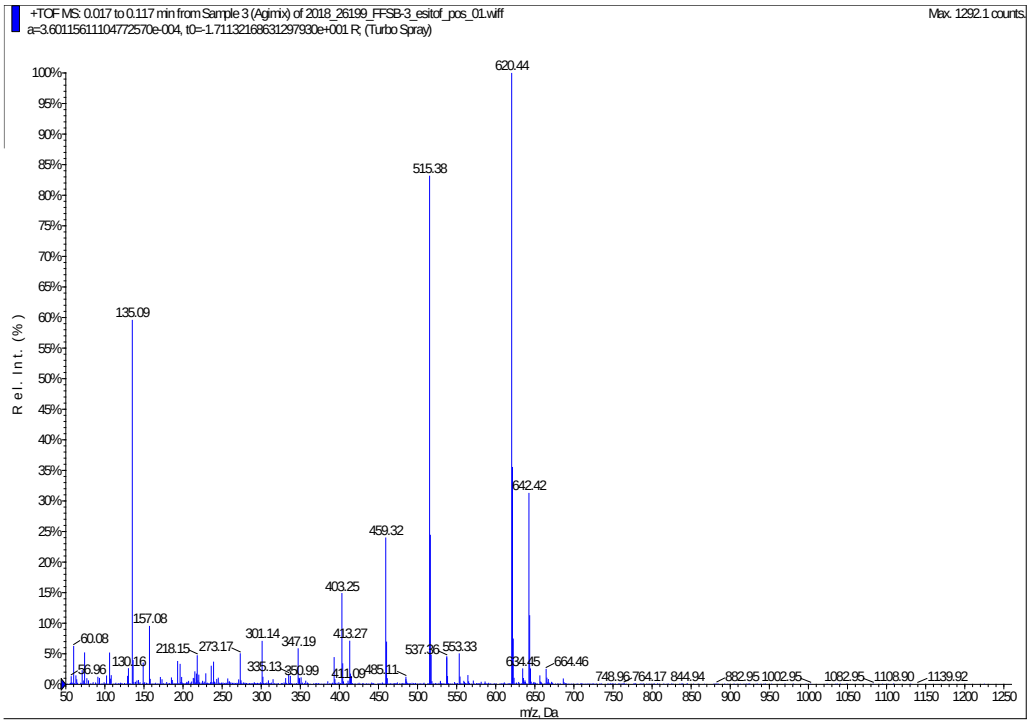
+TOF MS: 0.017 to 0.117 min from Sample 3 (Agimix) of 2018_26199_FFSB-3_esitof_pos_01.wiff
a=3.60115611104772570e-004, t0=-1.71132168631297930e+001 R, (Turbo Spray)
Max. 1292.1 counts.
Rel. Int. (%)
m/z, Da
620.44
515.38
135.09
642.42
459.32
403.25
157.08
60.08
301.14
347.19
413.27
218.15
273.17
537.36
553.33
634.45
664.46
56.96
130.16
335.13
360.99
411.09
485.11
748.96
764.17
844.94
882.95
1002.95
1082.95
1108.90
1139.92

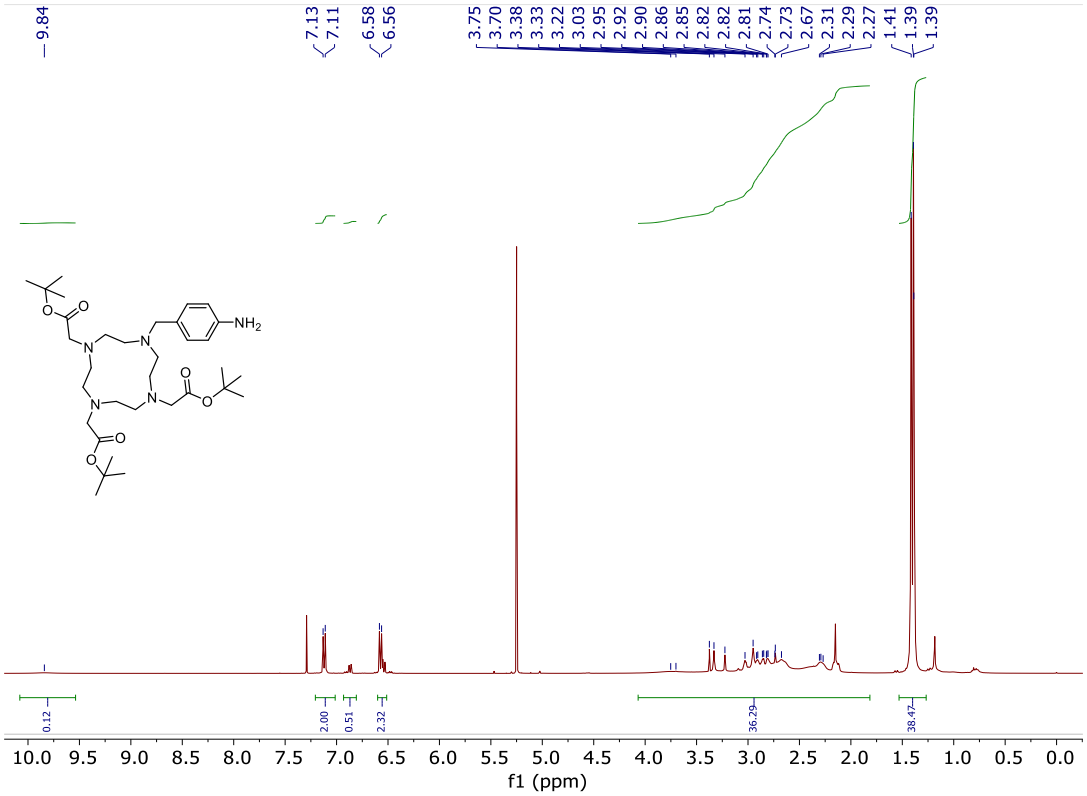
9.84
7.13
7.11
6.58
6.56
3.75
3.70
3.38
3.33
3.22
3.03
2.95
2.92
2.90
2.86
2.85
2.82
2.82
2.81
2.74
2.73
2.67
2.31
2.29
2.27
1.41
1.39
1.39
NH2
0.12
2.00
0.51
2.32
36.29
38.47
f1 (ppm)

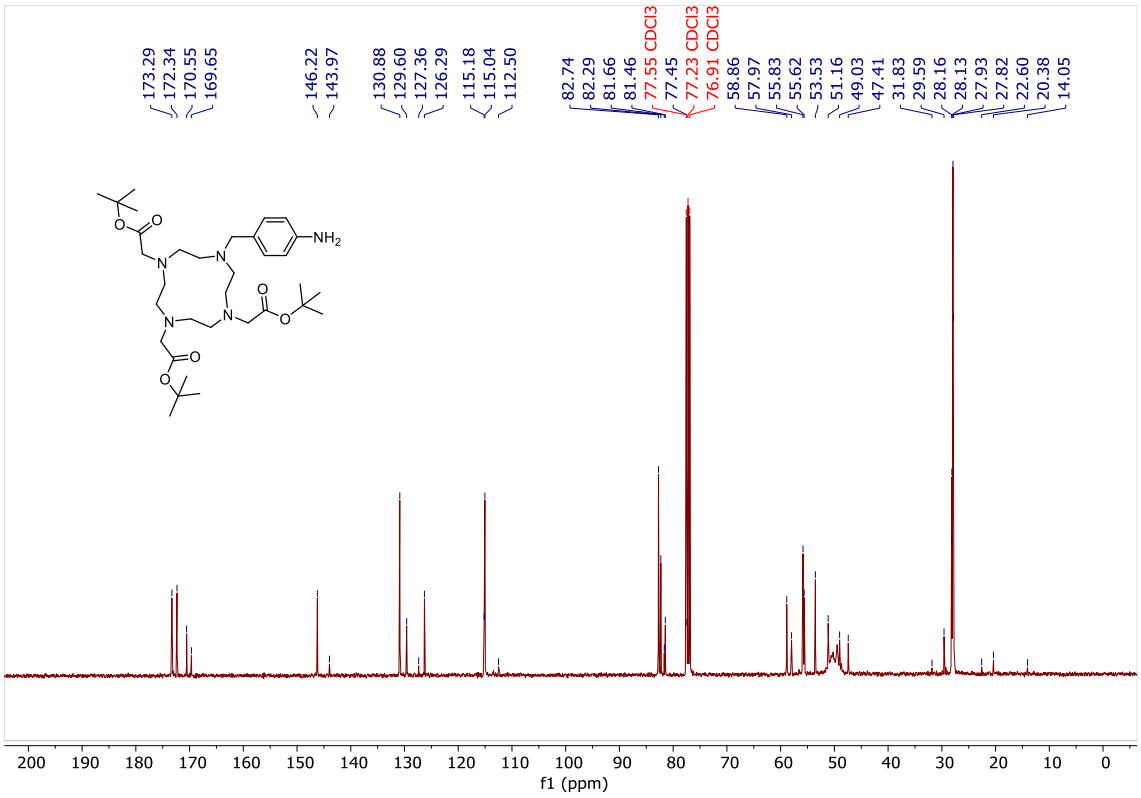
173.29
172.34
170.55
169.65
146.22
143.97
130.88
129.60
127.36
126.29
115.18
115.04
112.50
82.74
82.29
81.66
81.46
77.55 CDCl3
77.45
77.23 CDCl3
76.91 CDCl3
58.86
57.97
55.83
55.62
53.53
51.16
49.03
47.41
31.83
29.59
28.16
28.13
27.93
27.82
22.60
20.38
14.05
NH2
200 190 180 170 160 150 140 130 120 110 100 90 80 70 60 50 40 30 20 10 0
f1 (ppm)